

Cite this: *Phys. Chem. Chem. Phys.*, 2011, **13**, 10970–11001

www.rsc.org/pccp

PAPER

The gas-phase ozonolysis of α -humulene†M. Beck,^{‡a} R. Winterhalter,^{ab} F. Herrmann^a and G. K. Moortgat^{*a}

Received 3rd November 2010, Accepted 3rd March 2011

DOI: 10.1039/c0cp02379e

α -Humulene contains three double bonds (DB), and after ozonolysis of the first DB the first-generation products are still reactive towards O_3 and produce second- and third-generation products. The primary aim of this study consisted of identifying the products of the three generations, focusing on the carboxylic acids, which are known to have a high aerosol formation potential. The experiments were performed in a 570 litre spherical glass reactor at 295 K and 730 Torr. Initial mixing ratios were 260–2090 ppb for O_3 and 250–600 ppb for α -humulene in synthetic air. Reactants and gas-phase products were measured by *in situ* FTIR spectroscopy. Particulate products were sampled on Teflon filters, extracted with methanol and analyzed by LC-MS/MS-TOF. Using cyclohexane (10–100 ppm) as an OH-radical scavenger and by monitoring the yield of cyclohexanone by PTR-MS, an OH-yield of $(10.5 \pm 0.7)\%$ was determined for the ozonolysis of the first DB, and $(12.9 \pm 0.7)\%$ of the first-generation products. The rate constant of the reaction of O_3 with α -humulene is known as $k_0 = 1.17 \times 10^{-14} \text{ cm}^3 \text{ molecule}^{-1} \text{ s}^{-1}$ [Y. Shu and R. Atkinson, *Int. J. Chem. Kinet.*, 1994, **26**, 1193–1205]. The reaction rate constants of O_3 with the first-generation products and the second-generation products were, respectively, determined as $k_1 = (3.6 \pm 0.9) \times 10^{-16}$ and $k_2 = (3.0 \pm 0.7) \times 10^{-17} \text{ cm}^3 \text{ molecule}^{-1} \text{ s}^{-1}$ by Facsimile-simulation of the observed ozone decay by FTIR. A total of 37 compounds in the aerosol phase and 5 products in the gas phase were tentatively identified: 25 compounds of the first-generation products contained C13–C15 species, 9 compounds of the second-generation products contained C8–C11 species, whereas 8 compounds of the third-generation products contained C4–C6 species. The products of all three generations consisted of a variety of dicarboxylic-, hydroxy-oxocarboxylic- and oxo-carboxylic acids. The formation mechanisms of some of the products are discussed. The residual FTIR spectra indicate the formation of secondary ozonides (SOZ) in the gas phase, which are formed by the intramolecular reaction of the Criegee moiety with the carbonyl endgroup. These SOZ revealed to be stable over several hours and its formation was shown not to be affected by the addition of Criegee-radical scavengers such as HCOOH or H_2O . This suggests that in the ozonolysis of α -humulene at atmospheric pressures the POZ will decompose rapidly, and that a large fraction of the formed exited Criegee Intermediate will be stabilized to form stable SOZ, while the formation of OH-radicals *via* the hydroperoxide channel will be a minor process.

1. Introduction

The photooxidation of biogenic volatile organic compounds (BVOC) are primary sources of secondary organic aerosols (SOA),

which play an important role in atmospheric chemistry. The emissions of BVOCs largely exceed those of anthropogenic origin.² Most field and laboratory studies aimed at investigating the chemistry of BVOCs have been focussed on isoprene and monoterpenes ($C_{10}H_{16}$).^{2–4} On the other hand sesquiterpenes ($C_{15}H_{24}$), especially β -caryophyllene and α -humulene, play a very important role through their high reactivity in the atmosphere and their much higher aerosol formation potential.⁵

The estimated global BVOC emission rates are very uncertain. Kanakidou *et al.*⁶ reported that the emission of sesquiterpenes and other terpenes can be up to 5 times higher than estimated. Bonn *et al.*⁷ measured sesquiterpene mixing ratios of more than 100 ppt in ambient air in the summer and occasionally less than 1 ppt sesquiterpene in the winter. Also Kim *et al.*⁸

^a Max Planck Institute for Chemistry, Atmospheric Chemistry Department, P.O. Box 3060, D-55020 Mainz, Germany.
E-mail: geert.moortgat@mpic.de

^b Bavarian Health and Food Safety Authority, Pfarrstrasse 3, 80538 München, Germany

† This article was submitted as part of a collection following the 21st International Symposium on Gas Kinetics, held in Leuven in July 2010.

‡ Current address: Johannes Gutenberg-University, Institute for Inorganic and Analytical Chemistry, Duesbergweg 10–14, D-55128 Mainz, Germany.

used proton transfer reaction mass spectrometry (PTR-MS) to measure total sesquiterpene mixing ratios of 20 ppt in the summer in a deciduous forest. Some studies were performed to take into account the contribution of the type of plants, chemical speciation, light and the temperature dependence of the emissions.⁹ The sesquiterpenes emission of a variety of pine tree species was investigated by Helmig *et al.*¹⁰ They found that these can be up to 29% of the monoterpene emission, depending on species and temperature. In their study α -humulene was one of the ten most frequently emitted sesquiterpenes. Depending on the species of pine tree its fraction on the sesquiterpene emission can be higher than 10%.

Besides pine trees¹⁰ a large variety of plants emit sesquiterpenes and in particular α -humulene.¹¹ Different plants such as thale cress,¹² orange orchards,¹³ marsh elders,¹⁴ tobacco¹⁵ and sunflowers¹⁶ are proven to be α -humulene emitters. In hop, *Humulus lupulus*, α -humulene is a main constituent of the essential oil, and depending on the hop species it can consist up to 40% of the oil.¹⁷

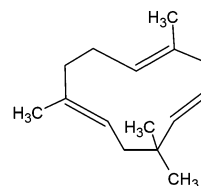
The reaction rate coefficient of α -humulene with ozone is very high ($1.17 \times 10^{-14} \text{ cm}^3 \text{ molecule}^{-1} \text{ s}^{-1}$) as compared to most monoterpenes such as α -pinene ($8.66 \times 10^{-17} \text{ cm}^3 \text{ molecule}^{-1} \text{ s}^{-1}$) and its lifetime under atmospheric conditions is estimated as 1 to 2 minutes.¹ Shu and Atkinson¹ also measured the rate constants for the reaction with OH-radicals ($2.9 \times 10^{-10} \text{ cm}^3 \text{ molecule}^{-1} \text{ s}^{-1}$) and with NO_3 radicals ($3.5 \times 10^{-14} \text{ cm}^3 \text{ molecule}^{-1} \text{ s}^{-1}$).

Griffin *et al.*⁵ showed that the aerosol formation potential of α -humulene photooxidation products is much higher than that of monoterpenes. Huff Hartz *et al.*¹⁸ performed a study of mono- and sesquiterpene ozonolysis in order to determine the CCN-activity of the products. They reported that products of sesquiterpenes ozonolysis are less CCN-active than those of monoterpenes ozonolysis. Moreover the results of α -humulene photooxidation studies performed in chamber experiments^{19,20} confirmed the important role of α -humulene in the formation of secondary organic aerosol (SOA). Griffin *et al.*⁵ reported a SOA yield of 32 to 85%, whereas Lee *et al.*²⁰ measured a SOA yield of $65 \pm 1\%$ with 53% relative humidity. Jaoui and Kamens¹⁹ measured particle size distribution and number concentration of the formed organic aerosols. These authors tentatively identified about 15 products besides some small molecules such as acetone and formaldehyde. The identified products were mostly formed by the oxidation of only one double bond (first-generation products). They used GC-MS for the identification of the major carbonyl products, whereas small products were identified by HPLC-MS using DNPH for derivatisation. Lee *et al.*²⁰ used PTR-MS to study the gas-phase products. Their results supported some products identified by Jaoui and Kamens.¹⁹ Lee *et al.*²⁰ observed acetaldehyde, formic acid, acetone and acetic acid but not formaldehyde, which was identified by Jaoui and Kamens.¹⁹

Dekermenjian *et al.*²¹ performed the ozonolysis of α -humulene to examine the chemical composition of the formed aerosol in a Teflon chamber using an excess of α -humulene and cyclohexane as an OH scavenger. They used a low pressure impactor (LPI) and FTIR spectroscopy. Particles were observed in all fractions between 0.05 to 1 μm . Ketones and aldehydes were found to be the dominant functional groups,

with 3.1 groups per average product molecule. They also determined 1.3 alcohol and 0.31 carboxylic acid groups per average product molecule.

α -Humulene contains three double bonds. After oxidation of the first double bond the first-generation products are still reactive. All the above-mentioned studies were focussed on the oxidation of one double bond. The further oxidation of the first-generation products has not been studied so far. Also the oxidation of the second-generation products, which still contain one double bond, has not previously been investigated.



In this study the ozonolysis of α -humulene with various ozone- α -humulene ratios was examined in a glass reactor. The primary aim consisted of analysing the products of the ozonolysis of α -humulene. Hereby the focus was laid on the carboxylic acids, which are supposed to have a high aerosol formation potential. Products of all three generations have been tentatively identified. Furthermore the reaction rate coefficients of O_3 with the first- and second-generation products have been determined. In addition, the OH yield of the ozonolysis of the first- and second double bond was measured. Finally the SOA yield was determined.

2. Experimental methods

An evacuable 570 l spherical glass reactor was used for the experimental investigations. The reactor is coupled with different analytical instruments and other devices. A FTIR-spectrometer is permanently attached (described in detail later), as well as a gas mixing device and an ozone generating system. SMPS (scanning mobility particle sizer) and PTR-MS (proton-transfer-reaction-mass spectrometer) are also coupled to the reactor. Various pumps enable us to reduce the pressure in the reactor to 6×10^{-6} Torr. The temperature was kept at $297 \pm 2 \text{ K}$ by the air conditioning of the room, whereas the pressure of the purified air in the reactor was maintained between 720 and 750 Torr. In some cases water vapour was added by passing air through a bubbler filled with 18 M Ω water (Elgastat) and quantified with a humidity sensor (Panametrics). In some experiments cyclohexane was added as an OH-radical scavenger. Formic and/or acetic acid were occasionally added as scavengers of the stabilized Criegee Intermediate (CI). These scavengers were used to elucidate the mechanism of the ozonolysis. The pressurised mixture of α -humulene in N_2 , as well as the used scavengers, was flushed *via* a transfer cylinder of 1.38 l into the reactor by the carrier gas N_2 . Because of the low vapour pressure of α -humulene it was necessary to repeat the flushing several times in order to introduce enough substance in the reactor. Ozone was generated externally by leading pure oxygen along an Hg Pen-Ray lamp. The mixing ratios of ozone, α -humulene and scavenger (except water, see above) were monitored by FTIR-spectroscopy. Three Teflon stirrers

Table 1 Number of experiments at various selected conditions in the ozonolysis of α -humulene

Added scavenger	Ratio ozone/ α -humulene		
	1–1.5	1.5–2.5	2.5 and higher
None	4	2	2
Acetic acid	1	2	2
Formic acid	2	3	3
Cyclohexane	3	2	1
Cyclohexane + formic acid	2	2	1
Formic acid + acetic acid	1	1	1
Water	3	4	4
Water + cyclohexane	3	4	5

in the reactor provided a rapid mixing of the reactants. A more detailed description of the experimental setup was given by the literature.^{22,23}

Initial mixing ratios of the reactants were varied between 250 and 600 ppb (1 ppb $\approx 2.3 \times 10^{13}$ molecule cm^{-3} at ambient temperature and pressure) for α -humulene and between 260 and 2090 ppb for ozone. The number of experiments at the various selected conditions of added scavengers is summarized in Table 1. The mixing ratios of the CI-scavengers formic and acetic acid were about 3 ppm, whereas those of H_2O varied between 6000 and 15000 ppm (equivalent to 20% to 55% relative humidity at the above conditions). Generally cyclohexane was added at a mixing ratio of about 300 ppm, sufficient to scavenge more than 97% of the formed OH-radicals.

2.1 FTIR spectroscopy

Long-path FTIR spectroscopy (Bruker IFS 28, 0.5 cm^{-1} resolution, 43.4 m path-length) was used to determine the mixing ratios of reactants and products. This spectrometer contained two detectors: a HgCdTe detector used for the spectral range 700–2000 cm^{-1} and an InSb detector for the range 2000–4000 cm^{-1} . In most experiments only the HgCdTe detector was used, because the main interesting features were obtained in its spectral range. For each spectrum 128 scans were averaged resulting in a time resolution of about 3 min for the acquisition of the data. For the kinetic experiments only 16 scans were averaged at the very beginning in order to realize a better time resolution. The calibration of HCOOH was described by Finkbeiner *et al.*²⁴ All other compounds have been calibrated by standard volumetric methods.

2.2 Proton-transfer-reaction mass spectrometry (PTR-MS)

A proton transfer reaction mass spectrometer (PTR-MS, Ionicon Analytik, Austria) was used for online measurements of volatile organic species. Lindinger *et al.*²⁵ for example described in detail the general principle of operation of the PTR-MS. The specific mass spectrometer used in this study has been successfully employed in numerous previous field²⁶ and laboratory²⁷ studies. For this study practically the same setup was used such as described in Herrmann *et al.*²⁷

A water-fed hollow cathode discharge source produced high concentrations of H_3O^+ ions (circa 5×10^6 ions cm^{-3}). These are introduced by a stable, regulated flow of ambient air (15 ml min^{-1}) into an ion/molecule reaction drift tube maintained at 50 °C and 2.2 mbar pressure. In order to increase time resolution and to minimise sample line residence time,

the ambient air flow of 15 ml min^{-1} was drawn from a faster stream (300 ml min^{-1}). Only compounds with a greater proton affinity than water can undergo efficient proton-transfer reactions with the H_3O^+ ions to produce protonated product ions in the drift tube. This means that a large section of OVOCs, aromatics and alkenes was protonated, while compounds with a lower proton affinity would not be protonated, especially such main constituents of the air, namely N_2 , O_2 and Argon. A quadrupole mass filter differentiated the ions based on their mass to charge ratio. An electron multiplier detected the selected ions. The concentration of a compound can be calculated by the known kinetics of the ion (H_3O^+)-molecule reaction or by independent calibration.

In this study only calibrations for cyclohexanone were performed in order to determine the OH-yield of the reaction (details will be given later). Several of these calibrations were performed during the experiments. The calibrations showed that the detector response was linear within the measured concentration range.

The ion source produces besides the needed H_3O^+ also other unwanted ions such as O_2^+ and NO^+ . Under these conditions cyclohexane, which is used in relatively high mixing ratios, is oxidised. Thus there is a permanent background at the mass of the protonated cyclohexanone. This background is very stable over time, and could easily be subtracted from our measurements. A poor detection limit for cyclohexane (5 ppb) is the result of the difference between this background signal and that obtained by sampling zero air. Because of the stability of the background, changes in the cyclohexanone signal could be readily and quickly registered, even at a level of the background plus three times its standard deviation (background: 5 ppb; standard deviation: 0.3 ppb).²⁷

2.3 Scanning mobility particle sizer (SMPS)

A scanning mobility particle sizer (SMPS, TSI 3936) monitored the aerosol concentration and its size distribution. The SMPS consists of an electrostatic classifier (TSI 3080) with a long differential mobility analyzer (LDMA; TSI 3081) and an ultra fine condensation particle counter (CPC; TSI 3025A) as a detector.

2.4 HPLC-MS

The generated aerosol particles were collected during 30–60 min on Teflon (PTFE) filters (45 mm diameter, 0.45 μm pore size). The filters were enclosed in a 7 cm^3 glass flask with 4 ml pure methanol added for extraction. After conditioning for at least two days, 3 ml of the solution was taken and concentrated to about 0.75 ml. The cooled sample solutions were concentrated by removing the methanol with a nitrogen stream. Small volatile compounds such as acetone could also be removed, but these compounds were not detectable with the used method. The exact volume was determined gravimetrically. A same volume of pure water was added, since pure methanol solutions cause a fronting problem in the used liquid chromatography. 100 μl of the solution was directly injected into the HPLC-MS system.

The HPLC system consisted of an autosampler (Series 200, Perkin Elmer, Norwalk, Connecticut, USA), a degasser and

a quaternary pump (Series 1100, Agilent Technologies, Waldbronn, Germany). The analytical column was a ReproSil-Pur C₁₈-AQ (250 mm × 2 mm id, 5 μm particle size) in a PEEK (poly-ether-ether-ketone) cartridge (Dr Maisch GmbH, Ammerbuch, Germany). The flow rate of the gradient elution was 400 μl min⁻¹. An eluent solution of 0.1% (v/v) formic acid in deionised water (eluent A) and acetonitrile (eluent B) was used. The gradient started with 100% A for 30 s, followed by a gradient from 100% A to 95% B during 20 min; thereafter the gradient turned back to 100% A in 3 min. The electrospray ionization in the negative mode (ESI⁻) was used as an ionization technique at 400 °C and an ionization voltage of -4 kV. This system was coupled to a hybrid mass spectrometer (LC-Triple Quad-MS/MS-TOF QSTAR, Applied Biosystems MDS-SCIEX, Toronto, Canada). This instrument combines tandem mass spectrometry (MS/MS) with the high mass resolution of a time-of-flight detector (TOF). The tandem mass spectrometry (MS/MS) selects ions with different mass-to-charge ratios and through collision with neutral gas molecules (here N₂) the ions dissociate in various fragments (also called CID, Collision-Induced Dissociation). The MS-system and its software can display the Total Ion Chromatogram (TIC) or a chromatogram of selected mass-to-charge ratios (XIC, eXtracted Ion Chromatogram).

The combination of the used gradient elution and the ionisation method has been optimised for the separation of carboxylic acids.²⁸ Thus organic compounds without any carboxylic group are nearly undetectable in the present concentrations used in this study.

Most products of the particle phase were only tentatively identified because the needed standards were not available. Due to the high resolution of the used mass spectrometer, mostly one elemental formula was obtained, which was conform to the ozone/α-humulene reaction. The functional groups could be identified by CID: carboxylic acids usually show the loss of CO₂ whereas aldehydes the loss of CO. For example the loss of CO₂ and water indicates the presence of a dicarboxylic acid or an oxo-carboxylic acid. With the knowledge of the elemental formula and the CID fragmentation pattern it was thus possible to identify the type of the compound observed. The resulting structures of the observed compounds were further deduced from the postulated reaction pathways of the α-humulene ozonolysis described later in detail. In addition the earlier described experimental setup of the dicarboxylic acids showed also the formation of sodium-adducts. This has been observed in other studies.²⁹ The sodium-adducts helped to differentiate between dicarboxylic acids and hydroxy-oxocarboxylic acids with the same elemental formula.

2.5 Chemicals

Sources of the chemicals (stated purities in parentheses) were as follows: cyclohexane (99.9%), formic acid (98%), acetic acid (98%), α-humulene (98%) from Sigma-Aldrich, Steinheim, Germany. All chemicals were of highest purity, commercially available and used without further purification.

3. Results and discussion

The main focus of this study was laid on the product identification and the determination of the reaction mechanism of the ozonolysis of α-humulene. As mentioned above FTIR-spectroscopy, PTR-MS and HPLC-MS were used for the detection of various products. Moreover the OH-radical yield was determined by PTR-MS. The use of a scanning mobility particle sizer (SMPS) allowed the quantification of the aerosol yield under various conditions.

Since α-humulene contains three endocyclic double bonds, the products can be classified into three generations. The ozonolysis of the first double bond (DB) leads to first-generation products, whereas the consecutive ozonolysis of the remaining DB of the first-generation products leads to second-generation products and so on. To produce a specific generation of products, different ozone/α-humulene-ratios were used.

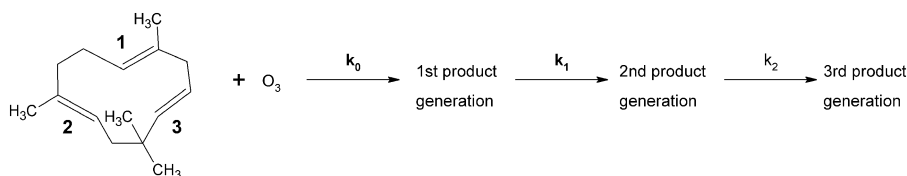
Further mechanistic insight can be obtained by using OH-radical- and CI-scavengers. Formic acid, acetic acid and water represented the CI-scavengers, whereas cyclohexane the OH-scavenger. A total of 58 experiments were conducted, as summarized in Table 1.

3.1 Reaction kinetics of the α-humulene + ozone reaction

Two of the three DB's of α-humulene (Scheme 1) have three alkyl substituents (DB 1 and 2) and are expected to have similar reactivities, whereas DB 3 with only two alkyl substituents has probably a different reactivity. By analogy to the reaction of ozone with small alkenes, the reaction rate constant of ozone with *trans*-2-butene (analogous to DB 3) is $1.9 \times 10^{-16} \text{ cm}^3 \text{ molecule}^{-1} \text{ s}^{-1}$, whereas the reaction rate constant of ozone with 2-methyl-2-butene (analogous of DB 1 and DB 2) is $4.0 \times 10^{-16} \text{ cm}^3 \text{ molecule}^{-1} \text{ s}^{-1}$.³⁰ Thus it can be assumed that DB 3 is the slowest reacting double bond. But the difference of the reaction rate constants is too small to establish which double bond will be preferentially attacked by ozone.

To determine the rate constants the following assumptions were made:

Here k_0 is the rate constant of the reaction of O₃ with the first double bond (DB 1) of α-humulene. This reaction leads to various products of the first generation. These first-generation products can further react with ozone and k_1 is the averaged



Scheme 1

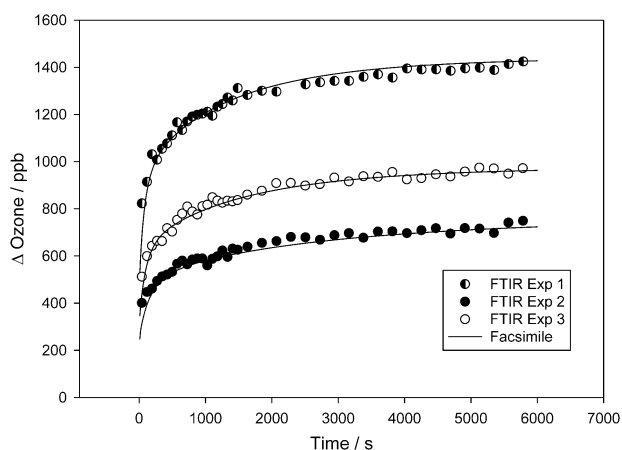


Fig. 1 Consumed ozone mixing ratio during the reaction of O_3 with α -humulene (α H), measured by FTIR; initial concentrations: Exp. 1 $[O_3]_1 = 2181$ ppb; $[\alpha H]_1 = 480$ ppb; Exp. 2 $[O_3]_2 = 1085$ ppb; $[\alpha H]_2 = 255$ ppb; Exp. 3 $[O_3]_3 = 1656$ ppb; $[\alpha H]_3 = 325$ ppb. For the simulations by Facsimile (full lines) the values $k_0 = 1.17 \times 10^{-14}$, $k_1 = 3.6 \times 10^{-16}$ and $k_2 = 3 \times 10^{-17}$ $\text{cm}^3 \text{ molecule}^{-1} \text{ s}^{-1}$ were used.

rate constant of all first-generation products. Analogously, this can be applied for the second-generation products with a rate constant k_2 . The formed OH-radicals may also attack α -humulene but this influence was neglected, since the OH-rate ($= k_{OH} \times [\text{humulene}]$) is much smaller than the O_3 -rate ($= k_{O_3} \times [\text{humulene}]$). As described later in detail the OH yield of the ozonolysis is about 10.5% for α -humulene and about 12.9% for the first-generation products. The ozone concentration was always much higher than the OH concentration.

The consumed ozone mixing ratios were plotted against reaction time for three experiments with different initial reactant mixing ratios (see Fig. 1). The amount of ozone was detected by FTIR. At the beginning of the reaction 16 scans were averaged for the generation of one spectrum, which resulted in a time resolution of less than 30 s. Later it was changed back to 128 scans per spectrum. In Table 2 the results of the three experiments and their initial mixing ratios are shown. The first constant k_0 was reported by Shu and Atkinson¹ as $1.17 \times 10^{-14} \text{ cm}^3 \text{ molecule}^{-1} \text{ s}^{-1}$. The program Facsimile³¹ was used to determine the rate constants of ozone with the first- and second-generation products using the known k_0 and varying k_1 and k_2 to obtain the best fit of the simulated ozone decay with the experimentally determined ozone time profile. The rate constants k_1 and k_2 were optimized so that the simulations of the three experimental ozone profiles gave the best fit with identical values for k_1 and k_2 . These simultaneous simulations of the three data set are shown in Fig. 1.

The rate constants derived for the second and third double bonds are $k_1 = (3.6 \pm 0.9) \times 10^{-16}$ and $k_2 = (3.0 \pm 0.7) \times 10^{-17} \text{ cm}^3 \text{ molecule}^{-1} \text{ s}^{-1}$, respectively. Under the conditions of excess O_3 over α -humulene, the initial attack reaction of O_3 with α -humulene with the very fast rate constant ($1.17 \times 10^{-14} \text{ cm}^3 \text{ molecule}^{-1} \text{ s}^{-1}$) will cause an instantaneous drop of the O_3 concentration, producing first-generation products. The rate of removal of these first-generation products is governed by the magnitude of k_1 , and can be observed by the curvature during the first 1000 s. The optimal simulations of the three data sets were obtained with an uncertainty of 25%. The slope of the tail of the curve ($t > 1000$ s) is controlled by the reaction rate constant k_2 . The overall uncertainty of k_2 is also estimated to be 25%. This was based on sensitivity runs where the magnitude of both k_1 and k_2 was varied independently by 25 and 50%.

The magnitude of the $k_1 = (3.6 \pm 0.9) \times 10^{-16} \text{ cm}^3 \text{ molecule}^{-1} \text{ s}^{-1}$ reflects the reaction rate constant of ozone with alkenes with increasing substitution around the $-\text{CH}=\text{C}-$ double bond (such as 2-methyl-2-butene 4.0×10^{-16} , *cis*-3-methyl-2-pentene 4.5×10^{-16} , *trans*-3-methyl-2-pentene 5.6×10^{-16} , *cis* + *trans*-3,4-dimethyl-3-hexene 4.5×10^{-16} , all in units $\text{cm}^3 \text{ molecule}^{-1} \text{ s}^{-1}$). The magnitude of $k_2 = (3.0 \pm 0.7) \times 10^{-17} \text{ cm}^3 \text{ molecule}^{-1} \text{ s}^{-1}$ is somewhat larger than some typical reactions of O_3 with substituted linear alkenes $\text{CH}_2=\text{CH}-$ (such as 3-methyl-1-butene 0.95×10^{-17} , 4-methyl-1-pentene 1.0×10^{-17} , 3,3-dimethyl-1-butene 0.39×10^{-17} , all in units $\text{cm}^3 \text{ molecule}^{-1} \text{ s}^{-1}$).³⁰

The rate constant k_0 is anomalously high, which cannot be explained by the alkyl substituents at the DB, since at least one type of DB is still present in the first generation products with a rather normal (expected) rate constant. A possible reason for the high rate constant of α -humulene and other cyclic sesquiterpenes might be the release of ring strain upon ozone attack on the DB.

At typical atmospheric ozone mixing ratios of about 30 ppb α -humulene has a lifetime of 2 min, whereas the averaged first-generation products have a lifetime of about 1 h and the second-generation products of about 12.5 h.

3.2 SOA-yield in the ozonolysis of α -humulene

Two groups of experiments were performed in order to determine the SOA-yield of the ozonolysis of α -humulene. The earlier described SMPS was used for this issue. No OH- or Cl-scavengers were added and the experiments were performed under dry conditions. Also no seed aerosol was used. Three experiments (Exp. 1 to 3) with α -humulene in excess and two experiments (Exp. 4 and 5) with 4-fold ozone excess were performed.

Table 2 Determined rate constants (in $\text{cm}^3 \text{ molecule}^{-1} \text{ s}^{-1}$) of α -humulene and initial mixing ratios

AU1409		AU1809		AU1909	
α -Humulene	480 ppb	α -Humulene	255 ppb	α -Humulene	325 ppb
Ozone	2182 ppb	Ozone	1085 ppb	Ozone	1656 ppb
k_0	1.17×10^{-14}	k_0	1.17×10^{-14}	k_0	1.17×10^{-14}
k_1	3.6×10^{-16}	k_1	3.6×10^{-16}	k_1	3.6×10^{-16}
k_2	3.0×10^{-17}	k_2	3.0×10^{-17}	k_2	3.0×10^{-17}

During the experiment with excess α -humulene, the aerosol number concentration reached a maximum within the first 10 min, with a particle diameter from 50 to 100 nm. At longer reaction times the particles grow in size, but their number gradually decreased due to coagulation and/or loss by deposition on the wall. Wall deposition rates depend on particle size, geometry of the reactor, turbulence in the chamber and charge distribution.^{32–34}

The wall loss in the glass reactor has been determined in a separate α -humulene experiment using excess ozone (typically 100 ppb α -humulene, 600 ppb ozone and 270 ppm cyclohexane) where the aerosol volume concentration was monitored at the end of the reaction ($t = 25$ min) for at least 30 minutes. The typical loss rate amounted to $5.6 \times 10^{-5} \text{ s}^{-1} = 0.20 \text{ h}^{-1}$, however with an uncertainty of 50%.^{35,36} In the present study it was assumed that the wall loss rate was constant during and between the performed experiments.

SOA yields were calculated from the aerosol mass occurring at the maximum number concentration, using a density of the aerosol particles of 1.0 g cm^{-3} . For the experiments using excess α -humulene, a 5% wall loss correction was applied, assuming a fast consumption of the sesquiterpene. For the experiments using excess ozone, wall loss corrections of 15% were applied, taking into account that the aerosol number concentration was monitored at about 30 minutes reaction time, when the sesquiterpene was almost completely converted.

As seen in Table 3 the corrected SOA-yield in the experiments with α -humulene excess varied between 14 and 17%. A high excess of ozone increased the yield to almost 45%. From the identification of the products by HPLC-MS (as described in detail below in Section 3.6), the different SOA yields can be explained by the degree of ozonolysis of the different double bonds. The SOA of the experiments with excess α -humulene should predominantly contain first-generation products. It could be assumed that these products have a relatively high molecular weight, mostly possessing two or more functional groups (see Section 3.6 in addition to an unknown number of unidentified products). All these products are expected to have a relatively low volatility and therefore have high SOA formation potential. On the contrary, the SOA of the experiments with ozone in excess contained mainly products of the second- and third-generation (second-generation products have a relatively long life-time, see above). The latter compounds have a relatively low molecular weight, but because of their functional groups they also possess a relatively low volatility.

The reason for the higher SOA-yield of the second- and third-generation cannot readily be explained. Donahue *et al.*³⁷ presented a study discussing the critical factors for SOA-yield from terpene ozonolysis. They showed that some competing

factors could affect the yield. A part of the increasing yield is caused by the higher oxygen atom to carbon atom ratio (for example C15-dicarboxylic acid **III** has a ratio of 4 to 15, whereas the ratio for C6-dicarboxylic acid **XIII** is 4 to 6). This oxygenation increased the absolute yield. Also the compounds are more polar and thus less volatile. But on the other hand carbon-carbon double bonds undergo ozonolysis and are therefore destroyed. This lowered the molecular weight and made the products more volatile. Donahue *et al.*³⁷ also mentioned the potential difference between gas phase and condensed phase oxidation subsequent to OH-attack, especially for cross-linking and oligomerization. Especially oligomerization could play an important role for the observed effect of higher SOA-yield for second- and third-generation products. Sadezky *et al.*²⁹ reported that main compounds of SOA originating from small alkenes-ozone reactions are oligomers. Pun and Seigneur³⁸ mentioned that the effect of oligomerization for the products of α -humulene and ozone is small because the monomers were already in the particle phase due to their low vapour pressure. As Kroll and Seinfeld³⁹ pointed out the volatility of products is very much influenced by the reactions of the formed peroxy- and oxy-radicals.

In the literature only values for the SOA-yield of α -humulene photooxidation^{5,20} are available. They reported SOA-yields between 32 and 85%. The photooxidation leads to a totally different chemistry. Therefore a comparison between those data and this study is very difficult. Winterhalter *et al.*²³ reported under compatible conditions SOA-yields for the ozonolysis of β -caryophyllene between 6 and 24% using excess sesquiterpene and no added scavenger. Thus it can be assumed that the SOA formation potential for the first-generation products of these two sesquiterpenes is similar.

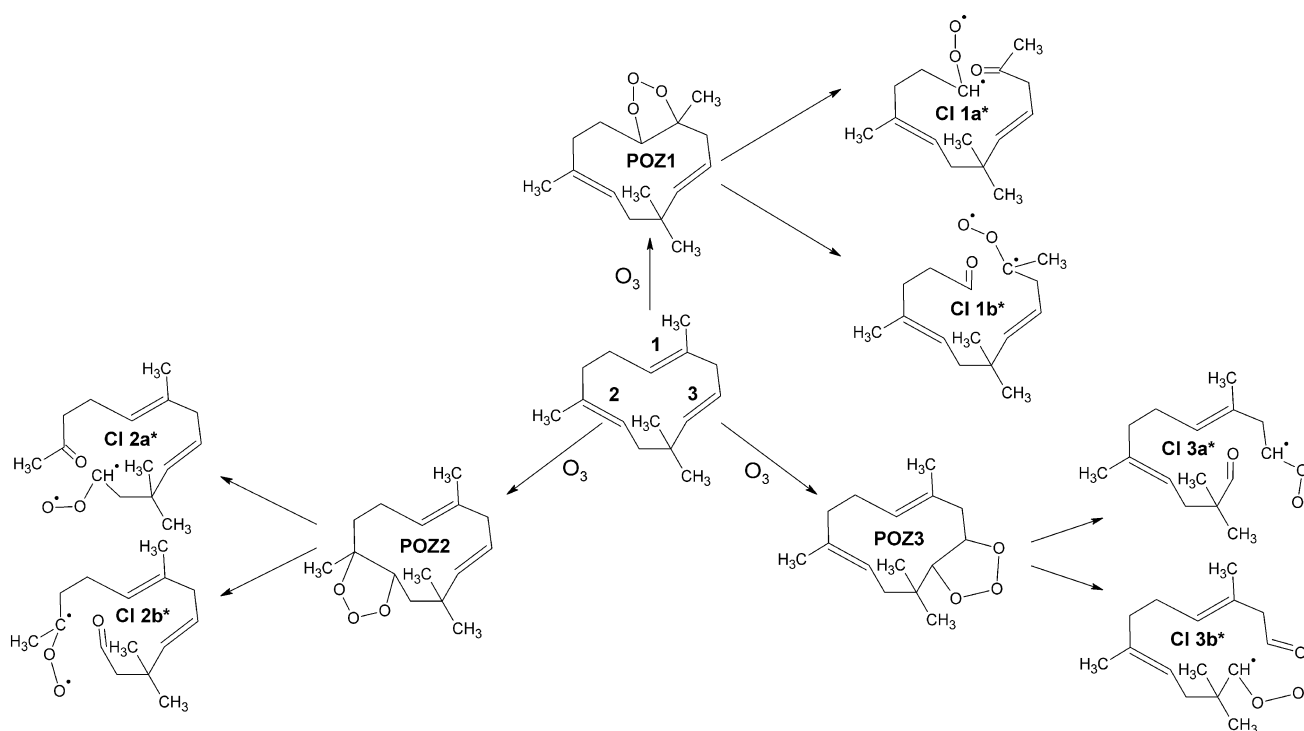
3.3 Reaction mechanism of the α -humulene + ozone reaction

Ozone addition at DB 1 and DB 2 leads to the two primary ozonides (**POZ 1** and **POZ 2**), whereas the less reactive DB yields **POZ 3**. Each POZ decomposes to two excited Criegee Intermediates **CI 1a*** and **CI 1b***, **CI 2a*** and **CI 2b***, **CI 3a*** and **CI 3b***, respectively (with *syn* and *anti* conformations a total of 12 CI). This is shown in Scheme 2.

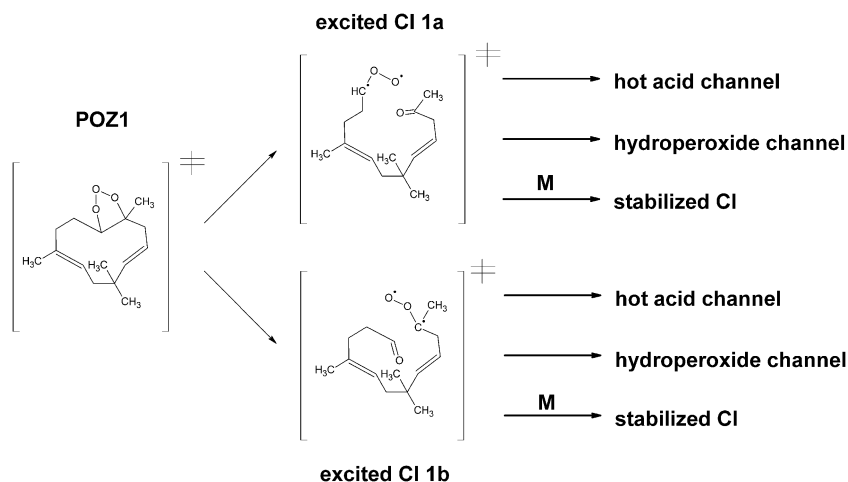
The excited CI has different reaction possibilities (see Scheme 3): it can react *via* the “hot acid channel”, also referred as “ester channel” or “dioxirane channel”,⁴⁰ or *via* the “hydroperoxide channel”, also referred as “vinyl hydroperoxide channel”. The “O-atom channel” is not important in most cases and was not considered.⁴⁰ The excited CI can also thermalize through collision with the carrier gas air, to form a stabilized CI (SCI). In this paper the Criegee Intermediate (carbonyl O-oxide) is

Table 3 SOA yield of α -humulene with various initial mixing ratios

Experiment	Reacted α -humulene in ppb	Ozone/reacted α -humulene ratio	SOA in $\mu\text{g m}^{-3}$ uncorrected	SOA in $\mu\text{g m}^{-3}$ corrected	SOA yield in %
Exp. 1	150	1.0	168	176	14
Exp. 2	150	1.0	200	210	17
Exp. 3	150	1.0	179	188	15
Exp. 4	270	4.0	880	1012	45
Exp. 5	410	4.0	1300	1495	44



Scheme 2



Scheme 3

represented as a biradical, but some theoretical calculation suggested a zwitterionic structure (*e.g.* Cremer *et al.*).⁴¹ Because of their relatively long lifetime, SCIs can bimolecularly react with scavenger molecules such as aldehydes, ketones, organic acids (*e.g.* formic and acetic acid) and H_2O .⁴²

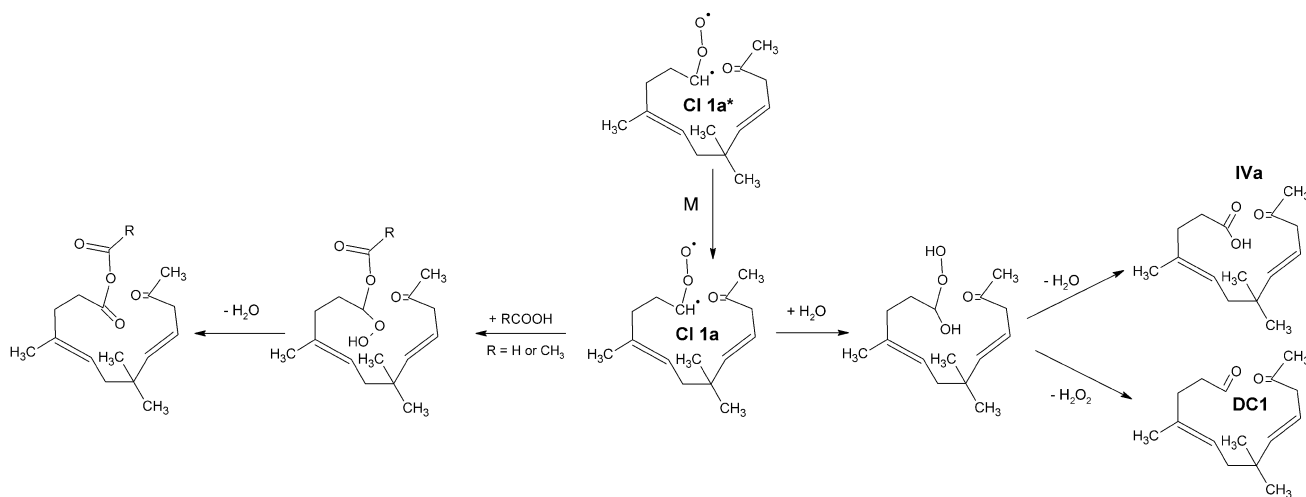
As shown as an example in Scheme 4, the SCI **CI 1a** can react with water as CI-scavenger to a dicarbonyl-compound (**DCI**) or to an oxocarboxylic acid (**IVa**, tentatively identified). Acids ($RCOOH$) as scavengers lead to the corresponding acid anhydrides.

Another possibility is the formation of internal secondary ozonides (**SOZ**). This intramolecular reaction is known to occur in the ozonolysis of cycloalkenes and was postulated by Chuong *et al.*⁴³ to occur if the excited Criegee Intermediates

have collisionally been stabilized. These authors showed through theoretical calculations that the formation of SOZ will be the dominant process for C15 alkyl-substituted cyclohexenes, which served as surrogate for sesquiterpenes. The SOZ formation and the pathways of both the hot acid and the hydroperoxide species will be described later in detail.

3.4 Mechanism of OH-formation and measurement of OH-yields

Every CI reacting through the hydroperoxide channel yields an OH-radical. The fraction of molecules, which entered this channel, depends on the molecule structure and needs to be experimentally determined for every different alkene reacting

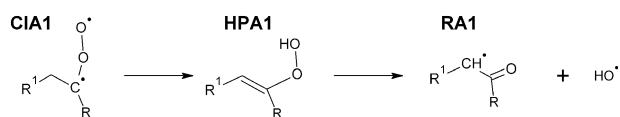


Scheme 4

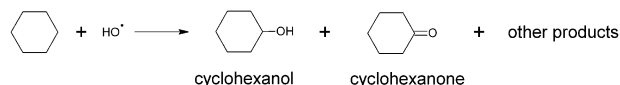
with ozone. The formation of OH is shown in Scheme 5 starting from a CI of a simple alkene (CIA1). The excited CI forms a hydroperoxide (HPA1) via transfer of an H atom in the α -position (1,4-hydrogen shift). This hydroperoxide can split off an OH-radical with the formation of a new radical (RA1).⁴⁰ The hydroperoxide channel and its products will be discussed later for the particular case of α -humulene.

A common method to determine OH-radical yields is the use of cyclohexane as an OH-scavenger. The OH-scavenging effect of cyclohexane is well known and explained in detail in the literature.⁴⁴ The reaction of cyclohexane with OH-radicals mainly leads to cyclohexanol and cyclohexanone,^{44,45} as seen in Scheme 6.

As described earlier, only cyclohexanone could be measured by PTR-MS. Therefore the relative yield of cyclohexanone has to be known. Unfortunately the yield of cyclohexanone depends on the initial compound undergoing ozonolysis. Atkinson *et al.*⁴⁴ reported a combined (cyclohexanol + cyclohexanone) yield of 55% for a series of monoterpenes, with a ratio of cyclohexanone/cyclohexanol between 0.8 and 1.4, depending on the terpene. For simple alkenes this combined yield is 50%.⁴⁶ Berndt *et al.*⁴⁵ measured for α -pinene a total yield of 60% and for (cyclohexanol + cyclohexanone) with a ratio of 1.0. For sesquiterpenes in general and α -humulene in particular there are no specific data in the literature about the combined yield of (cyclohexanone + cyclohexanol). Shu and Atkinson¹ reported only a cyclohexanone/cyclohexanol ratio of 2.02 for the reaction of the first double bond of α -humulene.



Scheme 5



Scheme 6

Since the results of Berndt *et al.*⁴⁵ and Atkinson *et al.*⁴⁴ are very similar and since the latter measured a series of terpenes, the value of the latter (55%) was used for calculation of the total (cyclohexanol + cyclohexanone) yield. The ratio of cyclohexanone/cyclohexanol for the calculation was taken from Shu and Atkinson.¹ Although these values are based only on the ozonolysis of the first double bond of a molecule, they were also used for the calculation of the OH-yield of the first-generation products.

The OH-yield of 22% from ozonolysis of the first DB was previously measured.¹ However, there are no data available for the OH-yield of the second DB. The used experimental and calculation methods to determine the yield of first and second DB were developed by Herrmann *et al.*²⁷ The initial mixing ratios of cyclohexane were about 10 ppm in order to scavenge about 80% of the formed OH-radicals. For the calculation of the reaction ratios, the OH reaction rate constants of Atkinson⁴⁷ for cyclohexane and Shu and Atkinson⁴⁸ for α -humulene were used.

The measured cyclohexanone mixing ratios have been corrected to 100% complete scavenging. Because of the excess of ozone, the slower second and the third DB were also attacked by ozone. As seen in Fig. 2 the OH-reaction with cyclohexane started very fast, causing initially a sudden formation of cyclohexanone. During the further progress of the reaction the formation of cyclohexanone slowed down. The time was calculated at which 95% of the first DB of α -humulene had reacted with ozone (marked in Fig. 2 with the left vertical black line). Unfortunately, in this relevant time period the PTR-MS was measuring the background, thus consequently the cyclohexanone yield was calculated by fitting the cyclohexanone signal before and after the background measurement. As can be seen in Fig. 2, even small uncertainties in the reaction time can affect the calculated yield. The same procedure was done to calculate the OH-yield of the second DB. It should be mentioned that this corresponds to the OH-yield of the first-generation products. By calculating the time at which 95% of the first-generation products had reacted, the initial ozone mixing ratios were corrected for the previously reacted ozone. The yield of the first DB was subtracted from the total measured yield at the

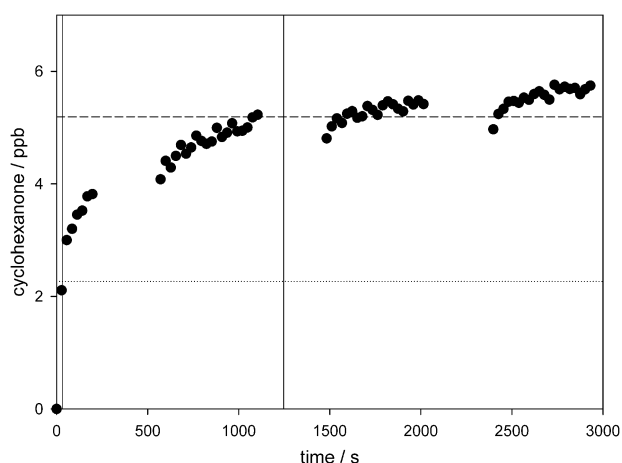


Fig. 2 Cyclohexanone yield used for calculation of the OH-yield. The dotted line marks the yield of the first double bond, the dashed line of the second double bond, whereas the vertical lines mark the reaction time when 95% of the respective double bond has reacted.

calculated reaction time.²⁷ It was assumed that the rate constant for the OH/first-generation products-reaction is in the same range as the OH/ α -humulene-reaction, so that the same amount of OH is scavenged by cyclohexane. Two experiments of this kind were performed for α -humulene (Table 4).

The OH-yield for the first double bond was 9.8 and 11.2% (average $10.5 \pm 0.7\%$) with an estimated uncertainty of 25%. The second double bond (average of all first-generation products) has a measured OH-yield of 12.3 and 13.6% (average $12.9 \pm 0.7\%$) with an estimated uncertainty of 30%. The measured OH-yield of 10.5% for the first double

bond is less than half the yield reported by Shu and Atkinson¹ (22%, using a small excess of α -humulene).

It is not obvious to explain the observed difference in OH yield. It is interesting to note that the sum of the OH yield of the first and second double bonds obtained in this study, $(10.5 \pm 0.7) + (12.9 \pm 0.7) = 23.5 \pm 0.7\%$, is in good agreement with 22% yield obtained by Shu and Atkinson.¹ The latter authors used a different combined yield of cyclohexanone and cyclohexanol (50% *versus* 55% in this study), but the same cyclohexanone/cyclohexanol ratio for the OH + cyclohexane reaction and another experimental method for detecting cyclohexanone. Also, in their experiments the ozone addition was made in 5 successive steps. As mentioned above the average reaction rate constant of O_3 with the first-generation products is relatively fast ($k_1 = 3.6 \times 10^{-16} \text{ cm}^3 \text{ molecule}^{-1} \text{ s}^{-1}$), so that it cannot be excluded that first-generation products have accumulated in the reactor between successive ozone additions, so that ozonolysis of these first-generation products took place, enhancing thus the OH yield.

3.5 Secondary ozonides

Secondary ozonides originate from the cyclisation of the stabilized Criegee Intermediates. The carbonyloxide-moiety of the CI-species reacts intramolecularly with the carbonyl-end to form an internal SOZ-group. Three different internal SOZ structures are possible (without considering any stereochemistry, see Scheme 7).

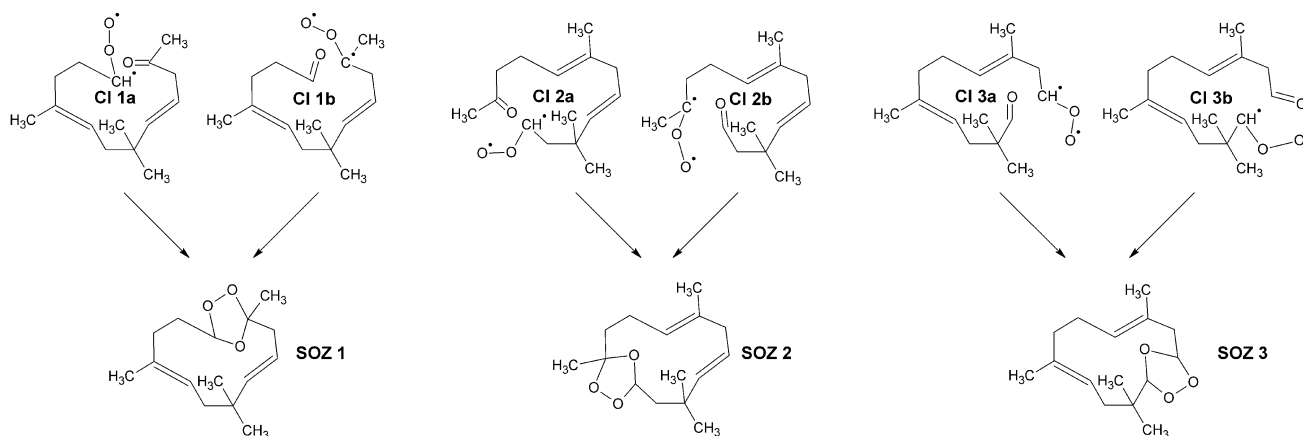
The formation of the internal secondary ozonides was detected in the gas phase by FTIR-spectroscopy. The FTIR spectra from experiments with less than a two-fold excess of ozone showed the characteristic absorptions of SOZ between 1100 and 1200 cm^{-1} (Fig. 3), which represent the range of the C–O stretching vibration. It is most probable that all three SOZ are formed. It is however suggested that the formation of **SOZ 1** and **SOZ 2** is favoured, because the three maxima in the relevant range of the FTIR-spectra are similar to those of the propene-SOZ⁴⁹ (having analogue DB 1 and 2). The analogue 2-butene-SOZ to **SOZ 3** has only one sharp maximum in this range.⁵⁰

As shown in Fig. 3 the influence of the CI-scavengers HCOOH, acetic acid and water is not significantly affecting

Table 4 OH-yield of first (1 DB) and second (2 DB) double bond

Experiment	OH-yield 1 DB in %	OH-yield 2 DB in %	Literature OH-yield 1 DB in %
Exp. 1	9.8	12.3	22 ^a
Exp. 2	11.2	13.6	
Average	10.5 ± 0.7	12.9 ± 0.7	22 ^a

^a From ref. 48.



Scheme 7

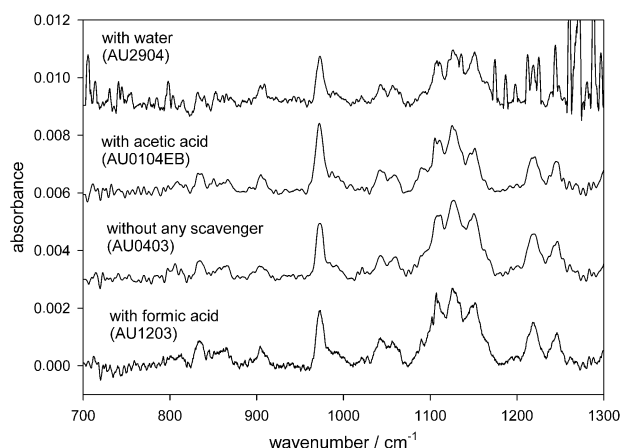


Fig. 3 FTIR-spectra of the α -humulene-SOZ under various experimental conditions (direct after ozone addition, similar initial α -humulene and ozone mixing ratios but different scavengers).

the magnitude of the spectra. This is an interesting finding because the suppression of SOZ-formation in the presence of CI-scavengers was shown in earlier studies, *e.g.* for β -pinene.⁵¹ Also the internal SOZ-formation of β -caryophyllene is partially suppressed by water and formic acid.²³ The reason for this non-suppressing behaviour is probably caused by the very fast intramolecular reaction of the CI-end with the aldehyde-end of the Criegee Intermediates.

The SCI formed by the ozonolysis of endocyclic alkenes was examined by Chuong *et al.*⁴³ for cyclohexene and a series of alkyl-substituted cyclohexenes. In this case the CI ozonolysis products are tethered and thus form a single disubstituted product, as in α -humulene. The authors disclosed that production of SOZ depends on the degree of collisional stabilization and the size of the Criegee Intermediates. Their theoretical calculations predicted that the stabilization of the CI leads to a dramatic transformation in the dominant oxidation pathway from an OH-radical-forming process at low carbon number to a SOZ-forming process at high carbon number. They concluded that at some carbon number between 8 and 15 (or something slightly smaller than monoterpenes and sesquiterpenes) SOZ formation dominated at all pressures. They also expected that any SCI formed from endocyclic sesquiterpenes would quickly cyclise to form SOZ, and therefore will not undergo bimolecular reactions with H_2O and other CI scavengers, as was observed in the case of α -humulene.

Another interesting aspect of the SOZs of α -humulene is their relative long lifetime. Under wet conditions about 40% of the SOZs remained after 140 minutes, while under dry conditions about 80% remained after 90 minutes. An excess of ozone decreased the yield of SOZ. More than a twofold excess of ozone destroyed all SOZs (Fig. 4). This means that no molecule with two ozonide-groups is formed or it is too unstable to be detected. The ozonolysis of first- and second-generation products did not seem to form SOZs in detectable amounts.

Some tentatively identified products can originate from the SOZs. The decomposition of the SOZs can be initiated by a hydrolysis or an ozonolysis in the reaction chamber or during the processing of the samples. Photolysis with UV-light has also recently been observed.⁵²

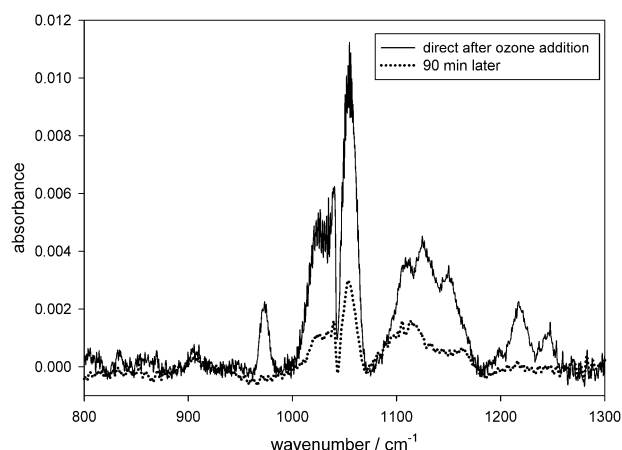


Fig. 4 FTIR-spectra of the formed α -humulene-SOZ directly after ozone addition and after 90 min, indicating the complete decay of the SOZ.

For example, the **SOZ 1** can react with water forming a molecule possessing an aldehyde (or a keto) group and a hydroxy-hydroperoxide group, as shown in Scheme 8. The latter compound can lose H_2O_2 and form an aldehyde with an additional oxo-group.^{53,54} Further oxidation of the aldehyde leads to the C15-oxocarboxylic acid **IVa**. Another possibility is that the hydroxy-hydroperoxide group loses water and **IVa** is directly formed.

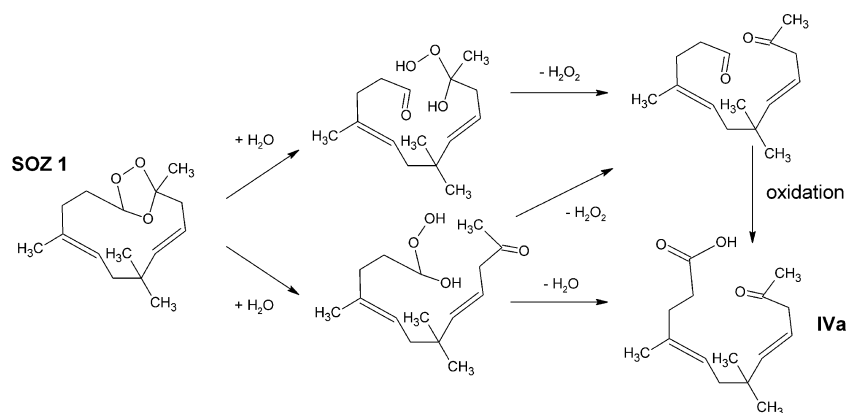
The oxocarboxylic acids **IVb** can be formed *via* similar pathways from the **SOZ 2**, and **IVc** and **IVd** from **SOZ 3**.

3.6 Tentatively identified products by HPLC-MS and CID

A summary of all tentatively identified oxidation products in the aerosol samples of α -humulene ozonolysis is given in Table 5. Some mentioned third-generation products were only detected in the gas-phase. Table 5 also presents the systematic IUPAC names (obtained with the software ACD/ChemSketch).

3.6.1 First-generation products. The six possible CIs lead to a multitude of theoretical products. Besides the three SOZs and their decomposition products mentioned above, the hot acid and the hydroperoxide channel can produce many other products. It should be noted that for most of the identified products more than one reaction pathway is possible, which could occasionally be proven by the different effects of the added scavengers. In total 5 products are tentatively identified, which are formed *via* the hot acid channel or also through the decomposition of the SOZs, while 24 products are obtained *via* the hydroperoxide channel. Fig. 5 to 7 show the possible products originating from the three POZs and a very rough estimation of the relative yield according to an excess α -humulene experiment without any scavengers. The relative yield is estimated assuming a similar sensitivity for the detection of the carboxylic acids and is indicated by the symbols L (large), M (medium) and S (small).

Hydroperoxide channel. The reaction pathway *via* the hydroperoxide channel leads to more theoretically and actually tentatively identified products than the hot acid channel. The hydroperoxide channel is the source of the OH-radicals that are formed during the ozonolysis of α -humulene. In the



Scheme 8

present study the yield of OH-radicals was determined as 10.5% for the first double bond and 12.9% for the second double bond. The products **IIa**, **IIb**, **IIIa–IIIh** and **Va–VIIb** (Table 5) are (most probably) formed through the hydroperoxide channel. The formation of the OH-radicals is shown below in Scheme 9 for **CI 1a** and **CI 1b** (with the same analogy for the other CIs). The CI forms an unsaturated hydroperoxide *via* a 1,4-hydrogen shift, which loses an OH-radical. New radical-intermediate species are thus formed from the different CIs: **CI 1a H1** from **CI 1a**, and **CI 1b H1** and **CI 1b H2** from **CI 1b**.

The C15-oxodicarboxylic acid **IIa** originates from the C15-radical **CI 1b H2** (see Scheme 10) and its analogue **IIb** was obtained from the corresponding **CI 2b**. An O₂ molecule adds to the radical **CI 1b H2** to form a peroxy radical. Two peroxy radicals can undergo a disproportionation reaction to form a molecule with an aldehyde group (or keto group, respectively) and one with an alcohol group. One of the newly formed molecules contains two aldehyde groups which can be oxidised to two acid groups. The formation pathway of product **IIa** is shown in Scheme 10. Analogous reactions occur for **IIb**.

Theoretically the third C15-oxodicarboxylic acid **IIc** should be also formed. But the extracted ion chromatograms XIC of m/z 281 ($M - H^-$) and m/z 303 ($M + Na - 2H^-$) only showed two different signals, which could be assigned to the possible structures. A significant loss of water was seen in both mass spectra using collision induced dissociation (CID). Thus it is assumed that only **IIa** and **IIb** were formed because **IIc** contains no H-atom in the β -position to a functional group, which would be necessary for the easy loss of water. For steric reasons it was assumed that **IIa** elutes earlier than **IIb** (both medium yield M).

First-generation products that contain only 14 or 13 carbon atoms are also formed *via* the hydroperoxide channel. All three possible C14-dicarboxylic acids (**Va–Ve**) were tentatively identified. As shown in Fig. 8 three not-completely-resolved signals in the extracted ion chromatogram (XIC) of m/z 253 ($M - H^-$) and m/z 275 ($M + Na - 2H^-$) display a correlation. The data of the CID experiments showed only loss of H₂O, CO₂ and the combination of the two. Thus only through steric reasons it can be assumed that the C14-dicarboxylic acids elute in the order **Va**, **Vb** and **Vc** (all medium yield M).

As an example the formation pathway of the dicarboxylic acid **Va** is shown in Scheme 11. Starting from **CI 1b H2** the

addition of O₂ leads *via* a C15-peroxy radical to a C15-oxy radical, which loses a formaldehyde molecule. The formed C14-radical adds O₂ forming a C14-acylperoxy radical, which can react with HO₂ either to form an acid (**VIb**) or a peroxyacid. The peroxyacid can undergo a Baeyer–Villiger-rearrangement yielding the dicarboxylic acid **Va**. The aldehyde group of the acid can be oxidised to the dicarboxylic acid **Va**. This postulated pathway is supported by the observed decreasing yield after the addition of the cyclohexane, because it destroyed one oxidizing species (OH-radicals). Therefore the OH-induced oxidation of the acid (**VIb**) is also a plausible formation pathway of the dicarboxylic acid **Va**.

The C14-oxocarboxylic acids **VIa–VIe** were also detected (all small yield S). A possible pathway for the formation of **VIb** was shown in Scheme 11. Analogue products are implied for the other oxocarboxylic acids. In the XIC of m/z 237 ($M - H^-$) various peaks are observed (Fig. 9). Three not-completely-resolved peaks (marked in the figure) seemed to be analogous to those of the corresponding C14-dicarboxylic acids. Thus the three peaks are supposed to belong to the C14-oxocarboxylic acids **VIa–VIe**. The CID spectra of all three oxocarboxylic acids mainly exhibit the loss of CO₂. Therefore, because of steric reasons the following elution-order can be estimated: first elute **VIa** and **VIb**, then **VIc** and **VId** and finally **VIe**.

Also both C13-dicarboxylic acids **VIIa** and **VIIb** were tentatively identified (both small yield S). In the XIC of m/z 239 ($M - H^-$) and m/z 261 ($M + Na - 2H^-$) one correlating signal was observed. The CID of m/z 239 showed the typical loss of CO₂, H₂O and a combination of both plus the loss of C₇H₁₀O₂. The structures of both dicarboxylic acids are consistent with this fragmentation pattern. In combination with the similar reactivity of the double bonds and the similar structure of the products (no additional methyl groups in the α -position), it can be assumed that both co-elute. The formation pathway is very similar as to the C14-dicarboxylic acids **Va–Ve** (all medium yield M). The starting point here is the C15-radical **CI 1b H1** or **CI 2b H1**, respectively. Instead of formaldehyde an acetyl radical is split. The intermediate radical W1 is formed by H-atom abstraction from an aldehyde group through *e.g.* an OH-radical, see Scheme 12. Alternatively the two aldehyde groups can be oxidised by OH-radicals (*via* W2). These assumptions were proposed because a decreasing yield

Table 5 Tentatively identified products of α -humulene ozonolysis

Product ID used in text	Structure	Molecular weight	Systematic abbreviation ^b	IUPAC nomenclature [terpene nomenclature ^a]
I		204	AU	(1E,4E,8E)-2,6,6,9-Tetramethylcycloundeca-1,4,8-triene [α -humulene]
IIa (M)		282	C15KDAc1	(4E,8E)-6,6,9-Trimethyl-2-oxododeca-4,8-dienedioic acid
IIb (M)		282	C15KDAc2	(4E,7E)-3,3,7-Trimethyl-11-oxododeca-4,7-dienedioic acid
IIc^c		282	C15KDAc3	(3E,7E)-3,7,10,10-Tetramethyl-2-oxoundeca-3,7-dienedioic acid
III (L)		268	C15DAc	(3E,7E)-3,7,10,10-Tetramethylundeca-3,7-dienedioic acid [α -humuladionic acid 10-acid]
IIIa (L)		268	C15AcKH1a1	(4E,8E)-2-Hydroxy-4,7,7-trimethyl-11-oxododeca-4,8-dienoic acid
IIIb (L)		268	C15AcKH1b1	(4E,8E)-10-Hydroxy-4,7,7-trimethyl-11-oxododeca-4,8-dienoic acid

Table 5 (continued)

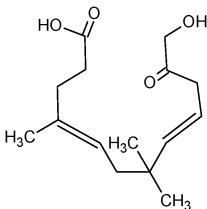
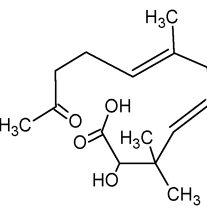
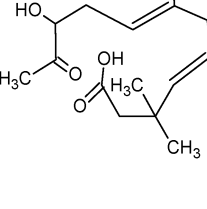
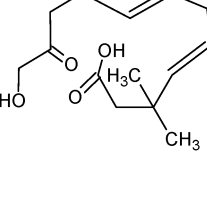
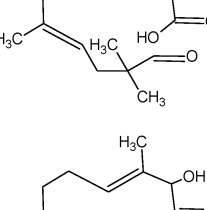
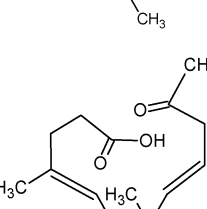
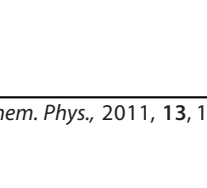
Product ID used in text	Structure	Molecular weight	Systematic abbreviation ^b	IUPAC nomenclature [terpene nomenclature ^a]
IIIc		268		
(L)			C15AcKH1b2	(4 <i>E</i> ,8 <i>E</i>)-12-Hydroxy-4,7,7-trimethyl-11-oxododeca-4,8-dienoic acid
IIId		268		
(L)			C15AcKH2a1	(4 <i>E</i> ,7 <i>E</i>)-2-Hydroxy-3,3,7-trimethyl-11-oxododeca-4,7-dienoic acid
IIIe		268		
(L)			C15AcKH2b1	(4 <i>E</i> ,7 <i>E</i>)-10-Hydroxy-3,3,7-trimethyl-11-oxododeca-4,7-dienoic acid
IIIf		268		
(L)			C15AcKH2b2	(4 <i>E</i> ,7 <i>E</i>)-12-Hydroxy-3,3,7-trimethyl-11-oxododeca-4,7-dienoic acid
IIIg		268		
(L)			C15AcKH3a1	(3 <i>E</i> ,7 <i>E</i>)-2-Hydroxy-3,7,10,10-tetramethyl-11-oxoundeca-3,7-dienoic acid
IIIh		268		
(L)			C15AcKH3a2	(4 <i>E</i> ,8 <i>E</i>)-10-Hydroxy-2,2,5,9-tetramethyl-11-oxoundeca-4,8-dienoic acid
IVa		252		
(S-M)			C15KAcl	(4 <i>E</i> ,8 <i>E</i>)-4,7,7-Trimethyl-11-oxododeca-4,8-dienoic acid [3- <i>seco</i> - α -humulaic-7-acid]

Table 5 (continued)

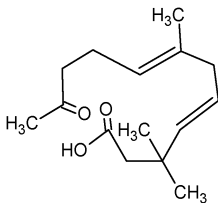
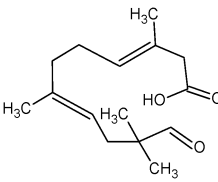
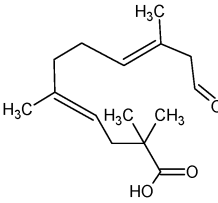
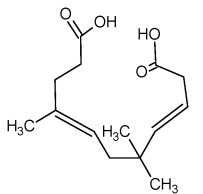
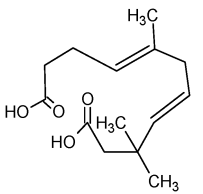
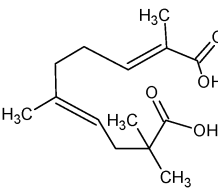
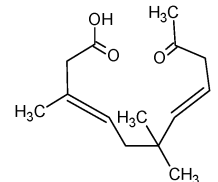
Product ID used in text	Structure	Molecular weight	Systematic abbreviation ^b	IUPAC nomenclature [terpene nomenclature ^a]
IVb		252	C15KAc2	(4 <i>E</i> ,7 <i>E</i>)-3,3,7-Trimethyl-11-oxododeca-4,7-dienoic acid [3-seco- α -humulaic-3-acid]
IVc		252	C15KAc3a	(3 <i>E</i> ,7 <i>E</i>)-3,7,10,10-Tetramethyl-11-oxoundeca-3,7-dienoic acid [α -humulalic 10-acid]
IVd		252	C15KAc3b	(4 <i>E</i> ,8 <i>E</i>)-2,2,5,9-Tetramethyl-11-oxoundeca-4,8-dienoic acid [α -humulalic 11-acid]
Va		254	C14DAc1	(3 <i>E</i> ,7 <i>E</i>)-5,5,8-Trimethylundeca-3,7-dienedioic acid
Vb		254	C14DAc2	(4 <i>E</i> ,7 <i>E</i>)-3,3,7-Trimethylundeca-4,7-dienedioic acid
Vc		254	C14DAc3	(2 <i>E</i> ,6 <i>E</i>)-2,6,9,9-Tetramethyldeca-2,6-dienedioic acid
VIa		238	C14KAc1a	(3 <i>E</i> ,7 <i>E</i>)-3,6,6-Trimethyl-10-oxoundeca-3,7-dienoic acid

Table 5 (continued)

Product ID used in text	Structure	Molecular weight	Systematic abbreviation ^b	IUPAC nomenclature [terpene nomenclature ^a]
VIb		238	C14KAc1b	(3 <i>E</i> ,7 <i>E</i>)-5,5,8-Trimethyl-11-oxoundeca-3,7-dienoic acid
VIc		238	C14KAc2a	(3 <i>E</i> ,6 <i>E</i>)-2,2,6-Trimethyl-10-oxoundeca-3,6-dienoic acid
VId		238	C14KAc2b	(4 <i>E</i> ,7 <i>E</i>)-5,9,9-Trimethyl-11-oxoundeca-4,7-dienoic acid
VIe		238	C14KAc3	(2 <i>E</i> ,6 <i>E</i>)-2,6,9,9-Tetramethyl-10-oxodeca-2,6-dienoic acid
VIIa		240	C13DAc1	(2 <i>E</i> ,6 <i>E</i>)-4,4,7-Trimethyldeca-2,6-dienedioic acid
VIIb		240	C13DAc2	(3 <i>E</i> ,6 <i>E</i>)-4,8,8-Trimethyldeca-3,6-dienedioic acid
VIII		214	C11DAc	(4 <i>E</i>)-2,2,5-Trimethyloct-4-enedioic acid
VIIIa		198	C11KAc2a	(4 <i>E</i>)-4,7,7-Trimethyl-8-oxooct-4-enoic acid

Table 5 (continued)

Product ID used in text	Structure	Molecular weight	Systematic abbreviation ^b	IUPAC nomenclature [terpene nomenclature ^a]
VIIIb		198	C11KAc2b	(4E)-2,2,5-Trimethyl-8-oxooct-4-enoic acid
IXa		184	C10KAc2a	(3E)-3,6,6-Trimethyl-7-oxohept-3-enoic acid
IXb		184	C10KAc3	(4E)-3,3-Dimethyl-7-oxooct-4-enoic acid
X		186	C9DAc	(3E)-5,5-Dimethylhept-3-enedioic acid
XI		186	C9AcKH1	(3E)-7-Hydroxy-3-methyl-8-oxooct-3-enoic acid
XIIa		172	C8AcKH1	(4E)-6-Hydroxy-5-methyl-7-oxohept-4-enoic acid
XIIb		172	C8AcKH2	(2E)-6-Hydroxy-2-methyl-7-oxohept-2-enoic acid
XIII		146	C6DAc	2,2-Dimethylbutanedioic acid
XIVa		130	C6KAc1	3,3-Dimethyl-4-oxobutanoic acid

Table 5 (continued)

Product ID used in text	Structure	Molecular weight	Systematic abbreviation ^b	IUPAC nomenclature [terpene nomenclature ^a]
XIVb		130	C6KAc2	2,2-Dimethyl-4-oxobutanoic acid
XV		114	C6DK	2,2-Dimethylbutanedial
XVI		116	C5KAc	4-Oxopentanoic acid
XVII		100	C5DK	4-Oxopentanal
XVIII		102	C4KAc	3-Oxobutanoic acid
XIX		86	C4DK	3-Oxobutanal

^a By ref. 19. ^b Cx = number of carbon atoms; K = keto-, oxo- or aldehyde-group; H = hydroxy-group; Ac = carboxylic acid-group; DX = two functional groups of X. ^c Substance was not detected. The letters L, M and S indicate the estimated relative yields of the first-generation products.

was observed caused upon addition of cyclohexane. The suggested reactions are displayed in Scheme 12.

The C15-hydroxy-oxocarboxylic acids can be also formed *via* the hydroperoxide channel. For the simplest possible reaction pathways eight possible compounds (**IIIa** to **IIIh**, all large yield L) could be formed. The formation of **IIIa** is shown as an example in Scheme 13. In the corresponding XIC of m/z 267 eight peaks were observed besides the peak of **III** (C15-dicarboxylic acid), see Fig. 10. The MS/MS experiments could not clarify the assignment of the peaks to the corresponding compounds; therefore no further assignment is made for these compounds.

Hot acid channel. The reaction pathway *via* the hot acid channel for **CI 1a** and **CI 1b** is shown in Scheme 14. **CI 2b** reacts analogously to **CI 1b**, all the other CIs analogously to **CI 1a**.

Only the C15-oxocarboxylic acid (**IVa**) was observed among these 5 possible products (Scheme 14). The detection of the other products shown in Scheme 14 was limited by the analytical technique, which only could detect carboxylic acids.

Also the analogous products **IVb–IVd** (shown in Table 5) were tentatively identified. Another first-generation product, which possibly originated mainly from the hot acid channel, is the C15-dicarboxylic acid **III** (α -humuladionic acid 10-acid). This product could be formed through the oxidation of **IVc** and/or **IVd**, as shown in Scheme 15.

The C15-dicarboxylic acid **III** could be tentatively assigned (large yield L). One corresponding signal in the XIC of m/z 267 ($M - H^-$) and m/z 299 ($M + Na - 2H^-$) was observed. The addition of the CI-scavengers formic and acetic acids caused a large increase of the yield (up to factor 4, see Fig. 11). The addition of the OH-scavenger cyclohexane decreased the yield significantly, whereas the addition of water had hardly any effect on the yield (Fig. 11). The increasing yield of **III** can be explained by an additional pathway. The scavenging acids can react with the stabilized **CI 3a** and **CI 3b** (C15 CIs) to form an anhydride, see for example **CI 3a** in Scheme 16. The resulting anhydride hydrolysed either in the chamber or more likely during the sample preparation. The decreasing yield caused by cyclohexane was attributed to the loss of one oxidative species, the OH-radical.

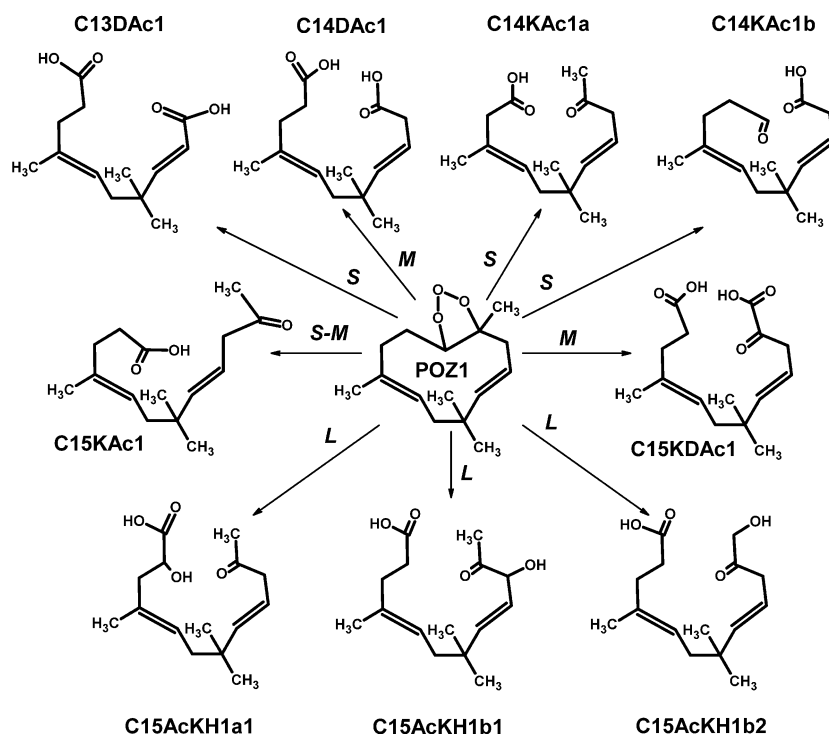


Fig. 5 Tentatively assigned products which originate from **POZ 1** (for symbols see Table 5). A very rough estimation of the relative yields is given by S for a small yield, M for a medium yield and L for a large yield.

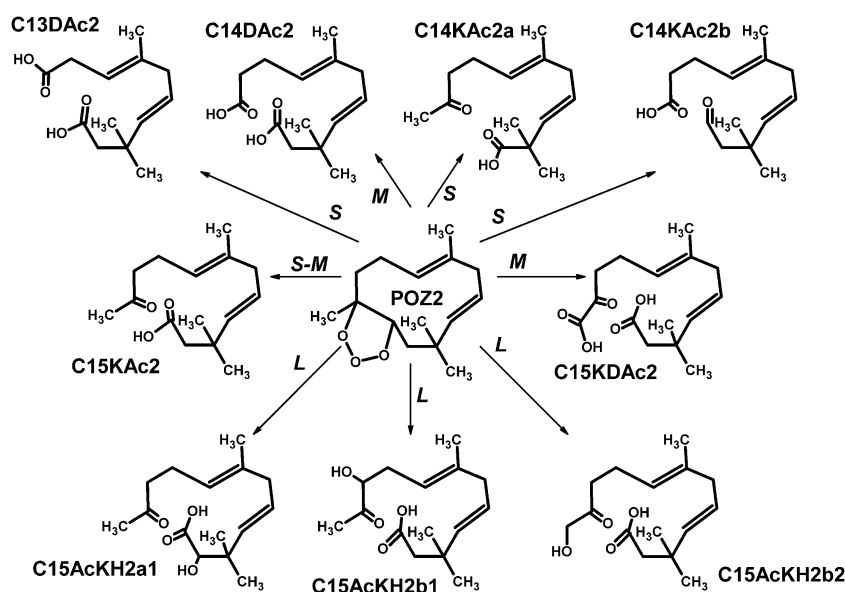


Fig. 6 Tentatively assigned products which originate from **POZ 2** (for symbols see Table 5 and Fig. 5).

The C15-oxocarboxylic acids **IVa–IVd** (all small to medium yield S–M) were observed in the XIC of m/z 251 ($M - H^-$), see Fig. 12, but the four signals are poorly resolved. As shown in Fig. 12 the effect of the addition of acetic acid as CI-scavenger is not the same for each of the oxocarboxylic acids. Therefore a relative quantification was not possible. It was also observed that the yield of the oxocarboxylic acids increased upon the addition of formic acid. The possible reason is explained analogously in Scheme 16. The formation of **IVa** is shown in

Scheme 14 as an example. Even a slightly higher excess of ozone decreased significantly the yield. This extreme sensitivity to the ozone- α -humulene ratio made it impossible to quantify the effect of cyclohexane. The eluting order of these compounds is assumed to be in the sequence **IVa** to **IVd**, because of steric effects. Furthermore, all five products can also originate from the decomposition of the SOZ as shown above.

It is interesting to note that 2/3 of the identified products of the first generation maintained their C15-skeleton.

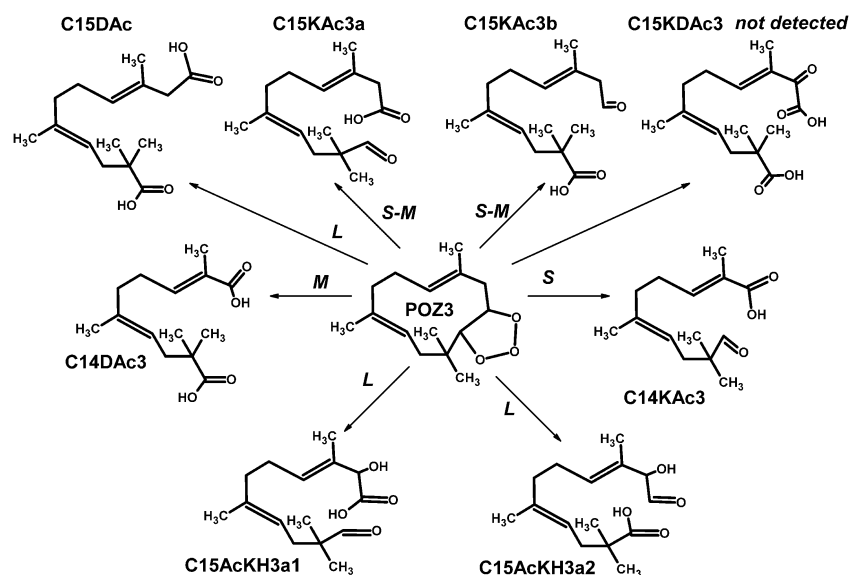
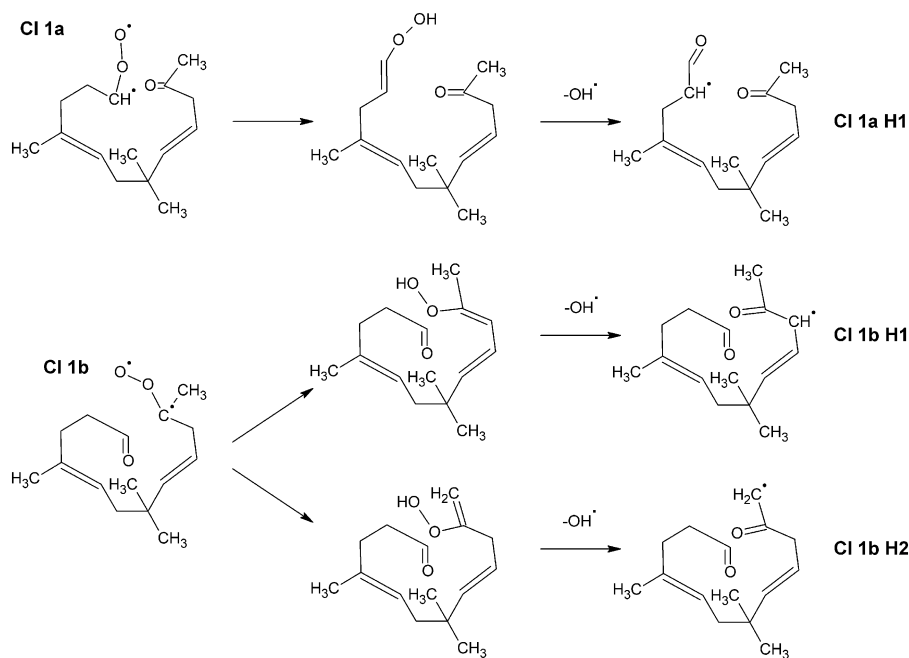
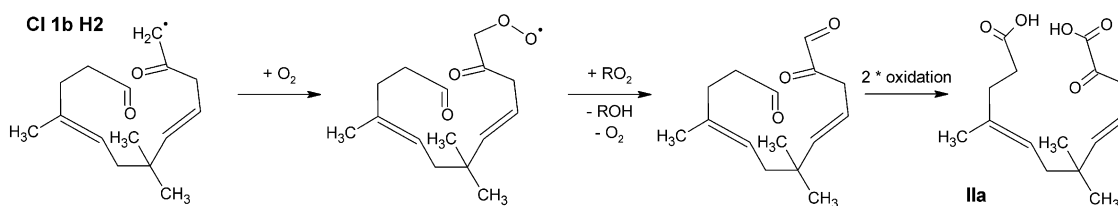


Fig. 7 Tentatively assigned products which originate from **POZ 3** (for symbols see Table 5 and Fig. 5).



Scheme 9



Scheme 10

The C15-hydroxy-oxocarboxylic acids (**IIIa** to **IIIh**) were observed with the largest yield, whereas the C15-oxodicarboxylic acids **IIa** and **IIb** were formed with an intermediate yield, all arising *via* the hydroperoxide channel. The identified

C15-dicarboxylic acid **III** was also formed with large yield *via* the hot acid channel, as well as the remaining C15-oxocarboxylic acids (**IVa** to **IVd**) however with a rather smaller yield (S-M). The remaining C14- and C13-products were

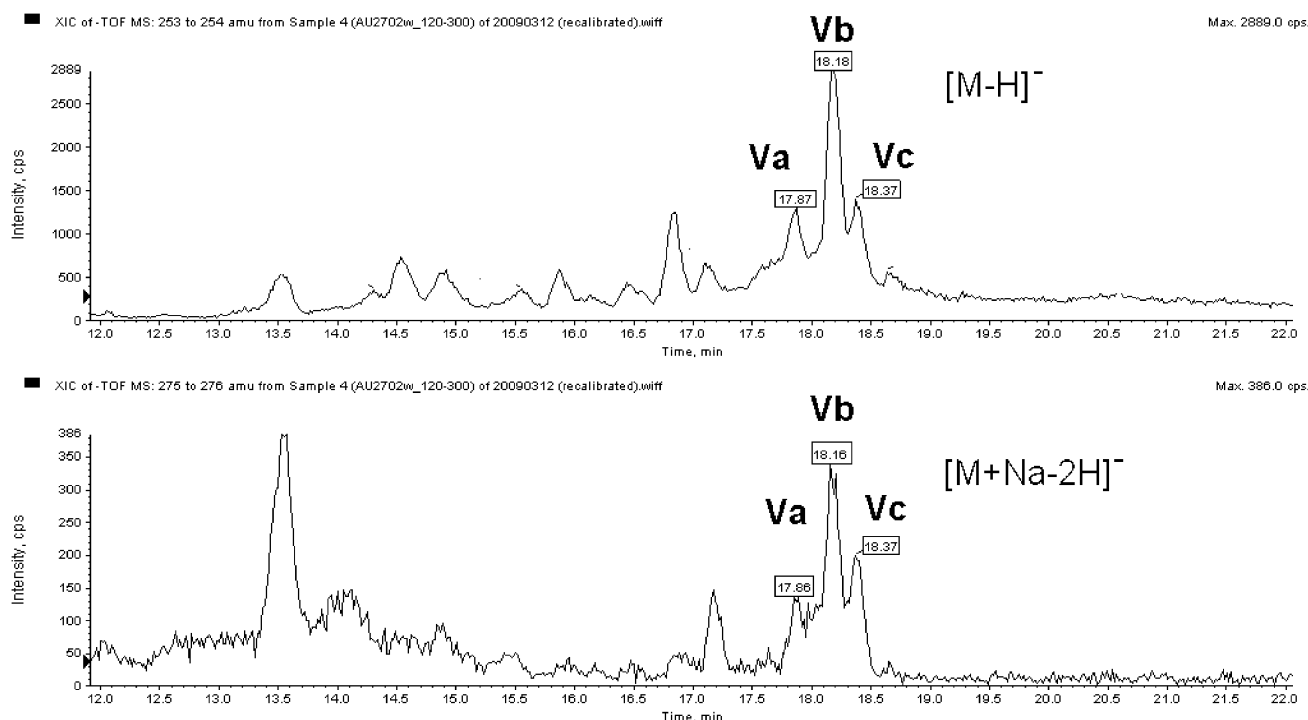
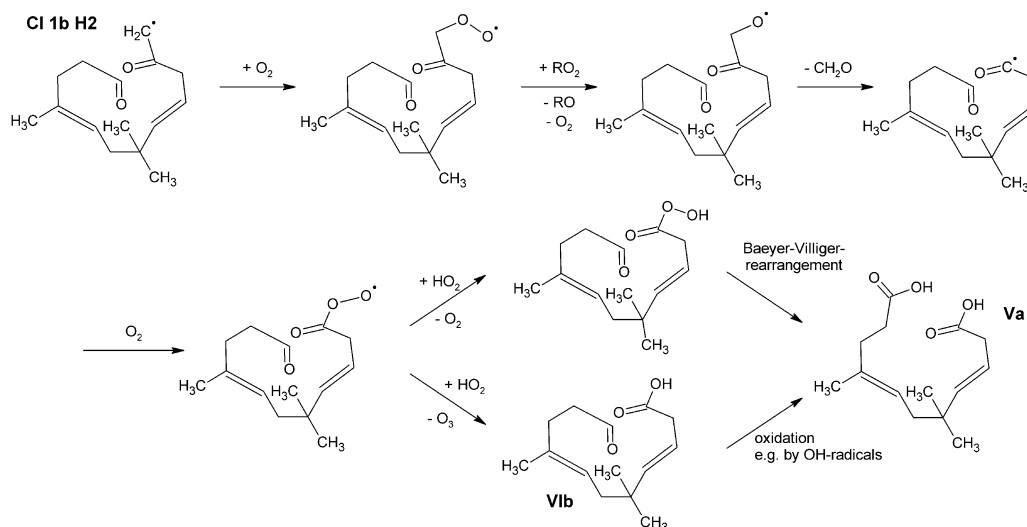


Fig. 8 Extracted ion chromatogram of m/z 253 and m/z 275 (C14-dicarboxylic acids **Va**, **Vb** and **Vc**).



Scheme 11

formed *via* the hydroperoxy channel with an intermediate (the C14 dicarboxylic acids **Va** to **Vc**) or small yield (the 14-oxo-carboxylic acids **Vla** to **Vle**, and the C13 dicarboxylic acids **VIIa** and **VIIb**). It is also observed that the relative yield of a specific type product is independent of its formation pathway. For example all C15-type III products (**IIIa** to **IIIh**) with large yield originate from all three POZs and do not seem to be affected by the initial attack of O_3 on the tri- or bisubstituted double bonds of α -humulene. This is also true for the C14-type VI (**Vla** to **Vle**) products with small yield.

3.6.2 Second-generation products. The molecules **VIII–XIIIb** (Table 5) represent these tentatively identified products of the

second generation. The ozonolysis of two double bonds is necessary to initiate their formation. Consequently, all the second-generation products possess one remaining double bond with 8 to 11 carbon atoms. The products of the second generation can originate from different possible pathways. For example, as demonstrated in Fig. 13, the C9-dicarboxylic acid **X** (C9DAc) can originate from 9 tentatively identified products. The relative yields of the second-generation products depend very much on α -humulene–ozone ratio, therefore even a rough estimation of the relative yield was not attempted.

In the XIC chromatogram of m/z 213 one peak was tentatively identified as the quasi-molecular ion of the C11-dicarboxylic acid **VIII**. It was also observed as the sodium-adduct at m/z 235.

XIC of -TDF MS: 237 to 238 amu from Sample 4 (AU2702w_120-300) of 2009031...

Max. 931.0 cps.

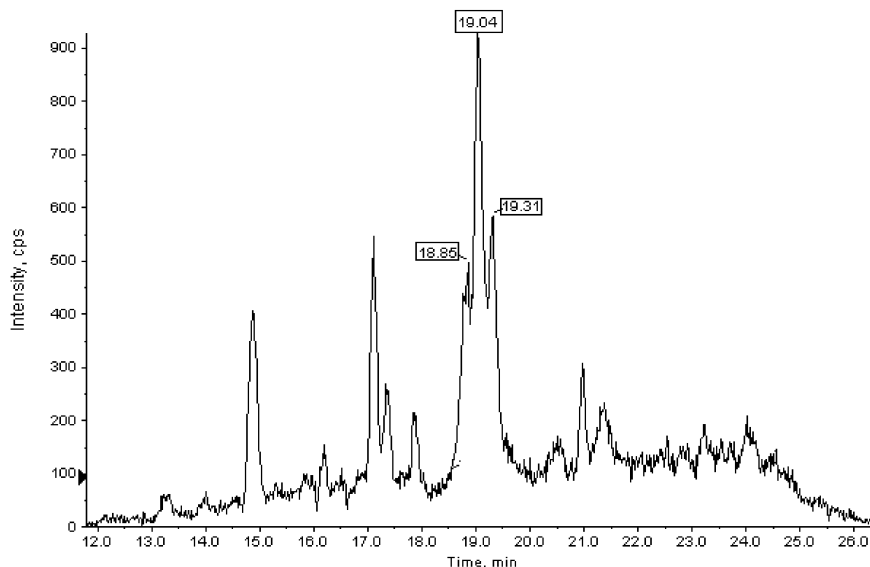
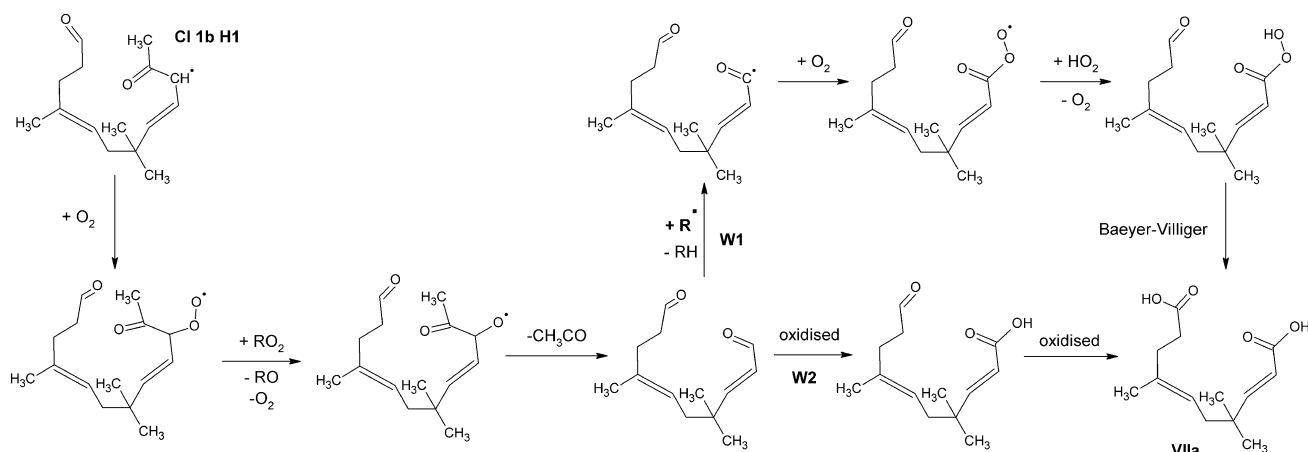
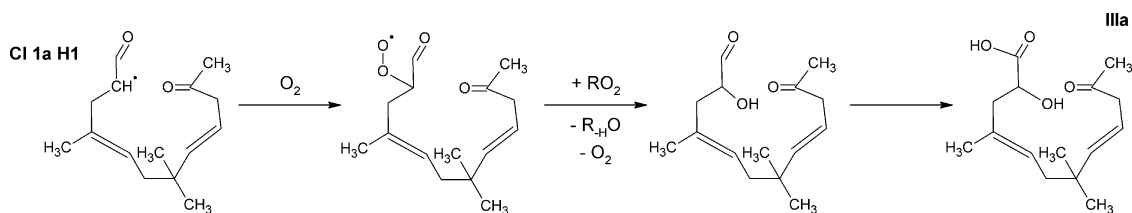


Fig. 9 Extracted ion chromatogram of m/z 237 (C14-oxocarboxylic acids **VIa** to **VIe**).



Scheme 12



Scheme 13

The CID experiment with 25 eV collision energy showed the loss of CO_2 , H_2O and a combination of both. Different pathways are thinkable to form **VIII** (Scheme 17). The simplest one is the first-generation CIs reacting through the hot acid channel to the C15-oxocarboxylic acids **IVa** or **IVd**. Upon ozonolysis of the corresponding second double bond resulting in the formation of CI (**C11 CII**), which can further react through the hot acid channel to form the C11-dicarboxylic acid **VIII**, the

C11 CII can be stabilized and react with a CI-scavenger. Another pathway is the oxidation of the C11-oxocarboxylic acids **VIIIa** and **VIIIb**. The last two possibilities are supported by the decreasing yield of **VIII** in the case of cyclohexane addition and the increasing yield in the case of formic acid or water addition (see Fig. 14). Thus it can be concluded that the C11-dicarboxylic acid **VIII** is formed by the different explained pathways, as is demonstrated in Scheme 17.

■ XIC of m/z 267 from Sample 4 (AU2702w_120-300) of 20090312 (recalibrated).wiff

Max. 9711.0 cps.

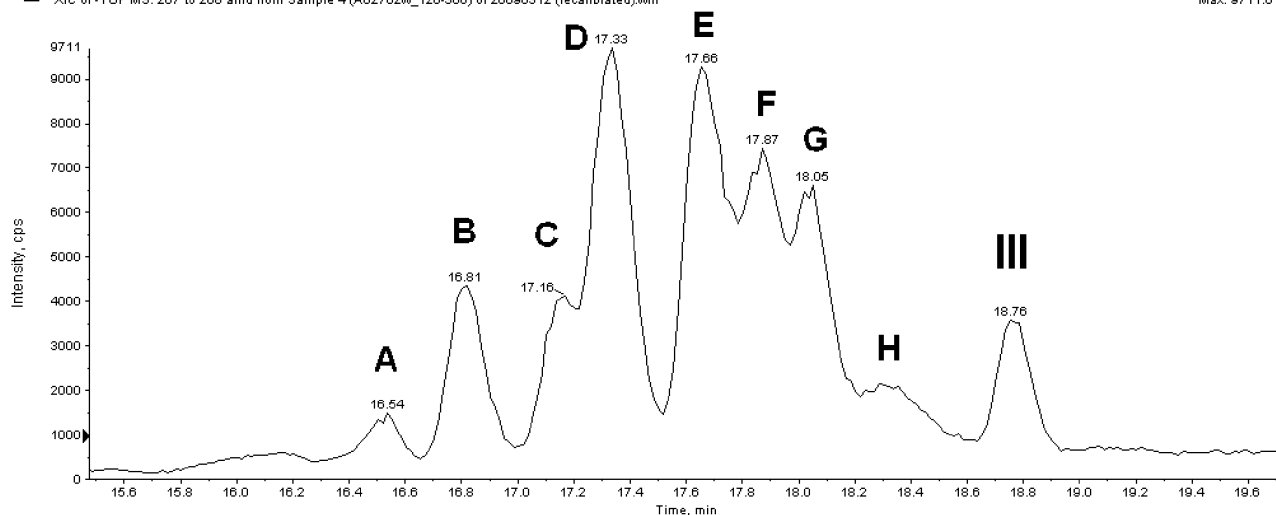
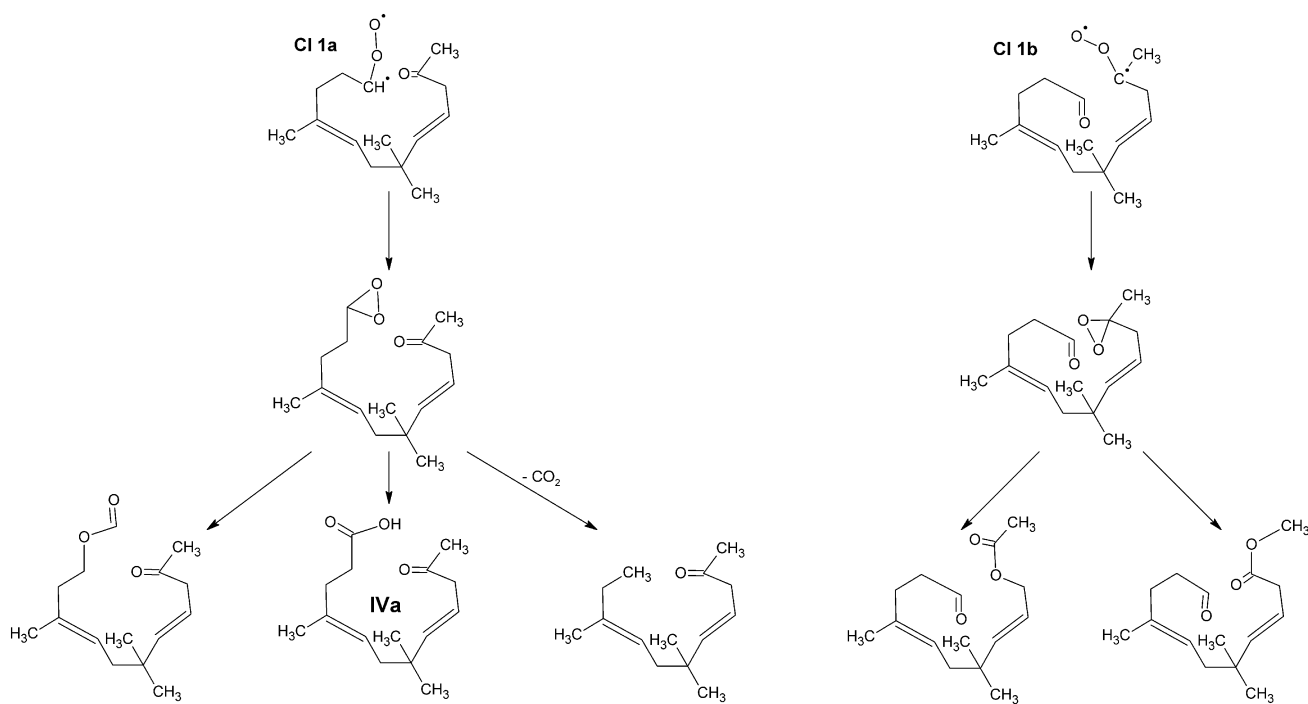
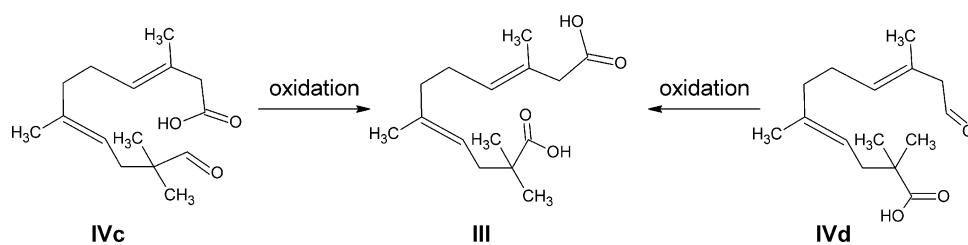


Fig. 10 XIC of m/z 267. Peaks A–H representing the assumed C15-hydroxy-oxocarboxylic acids **IIIa** to **IIIh**. (The labelled letters have no correlation with the sequence of the products assigned in Table 5.)



Scheme 14



Scheme 15

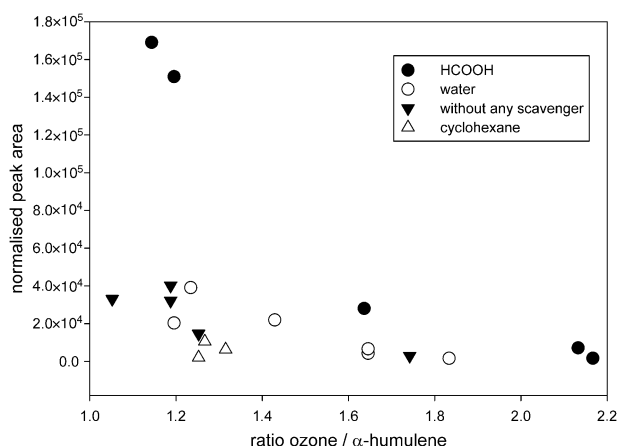
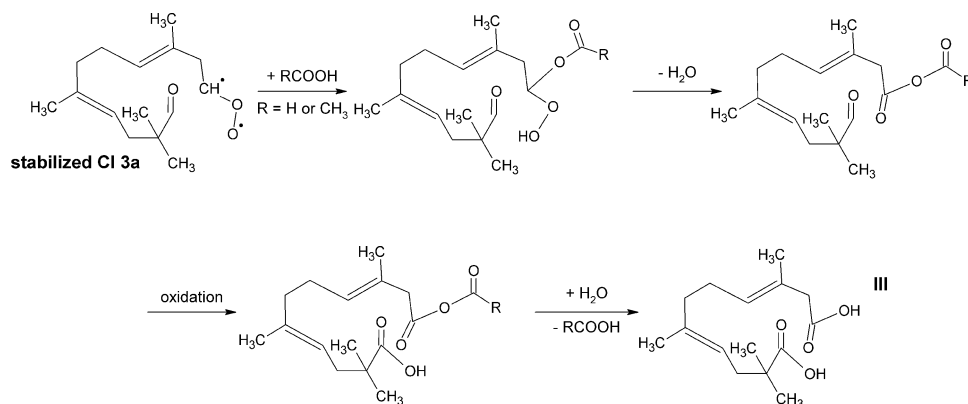


Fig. 11 Relative yields of III (C15-dicarboxylic acid) under various conditions.

Also evidence for the existence of the corresponding C11-oxocarboxylic acids **VIIIa** and **VIIIb** was seen in the XIC chromatogram of m/z 197. The exact mass to charge ratio correlated to the correct molecular formula. All fragments of the CID experiment can only be explained if **VIIIa** and **VIIIb** are assumed to co-elute (see Fig. 15 and 16). The CID mass

spectra of m/z 197 show the loss of CO_2 , followed by the loss of a methyl group, H_2O , CO and acetaldehyde. The products **VIIIa** and **VIIIb** can easily lose CO_2 and CO , but the elimination of the CH_3 radical and acetaldehyde is more favourable for **VIIIa** than for **VIIIb**, whereas the loss of H_2O is only possible for **VIIIb** (Fig. 16). The CI-scavengers formic and acetic acids increased the yield, whereas cyclohexane decreased it. Also the assertions for these effects are identical as for **VIII**. The retention time of the C11-oxocarboxylic acid **VIII** is about 2 min longer than for the C11-oxocarboxylic acids (**VIIIa** + **b**). Under the used HPLC conditions it would be expected that an aldehyde eluted later than the corresponding acid, but the observed trend (aldehyde elutes earlier than acid) has been mentioned in the literature under various conditions for different similar “couples”.⁵⁵

Two peaks were observed in the XIC chromatogram of m/z 183. The exact mass-charge-ratio of both peaks in combination with the structure of α -humulene indicated that they correlated with C10-ketocarboxylic acids. The CID spectra of the peak with the shorter retention time, as seen in Fig. 17, showed besides the typical $\text{M}-\text{H}-\text{CO}_2^-$ -fragment also the loss of CH_3COOH and the combined loss of CO_2 and CO . Therefore the most probable structure is the C10-oxocarboxylic acid **IXa**. The other possibility for the molecular formula is the



Scheme 16

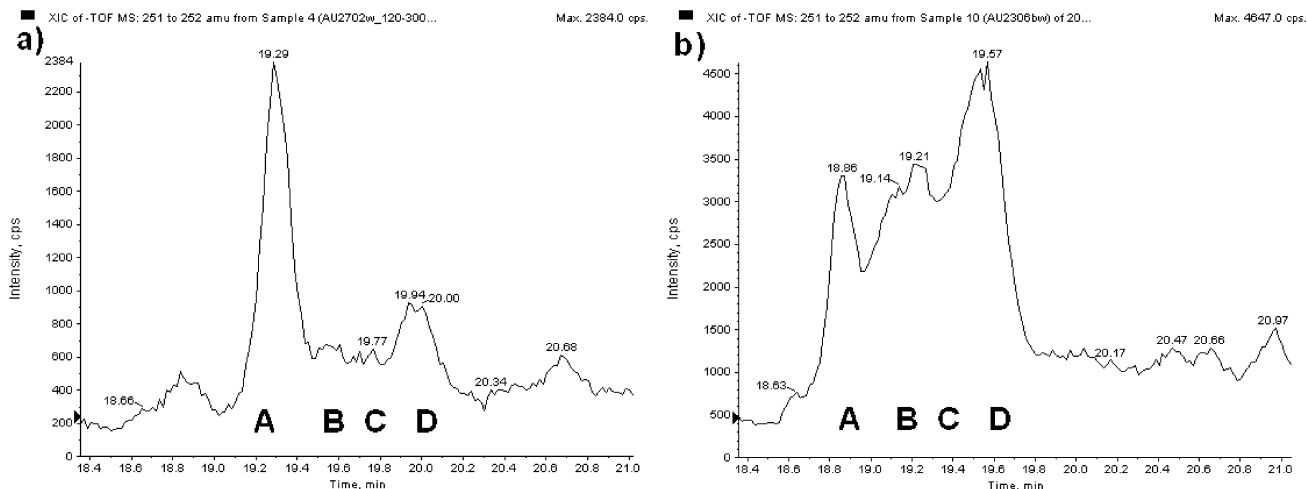


Fig. 12 XIC of m/z 251 (C15-oxocarboxylic acids **IVa** to **IVd**) (a) without scavenger, (b) with CI-scavenger acetic acid.

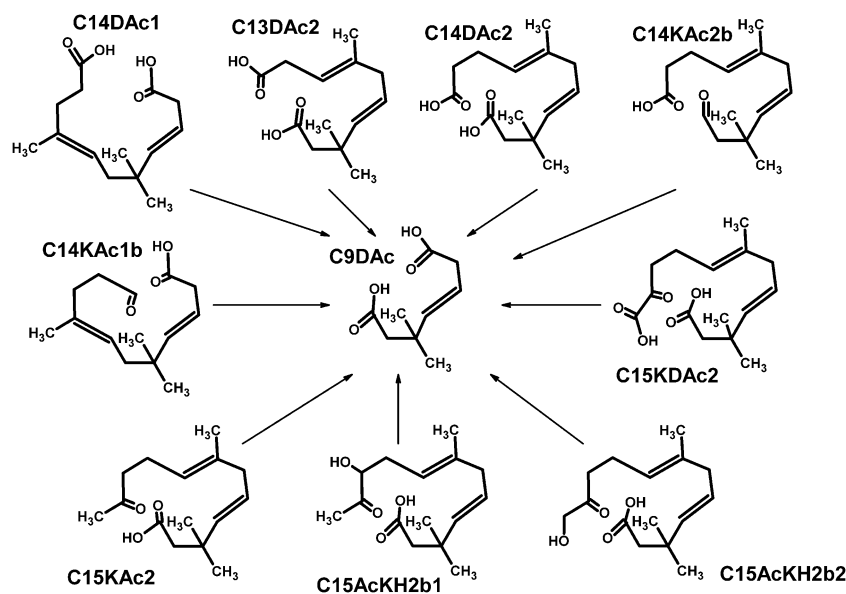
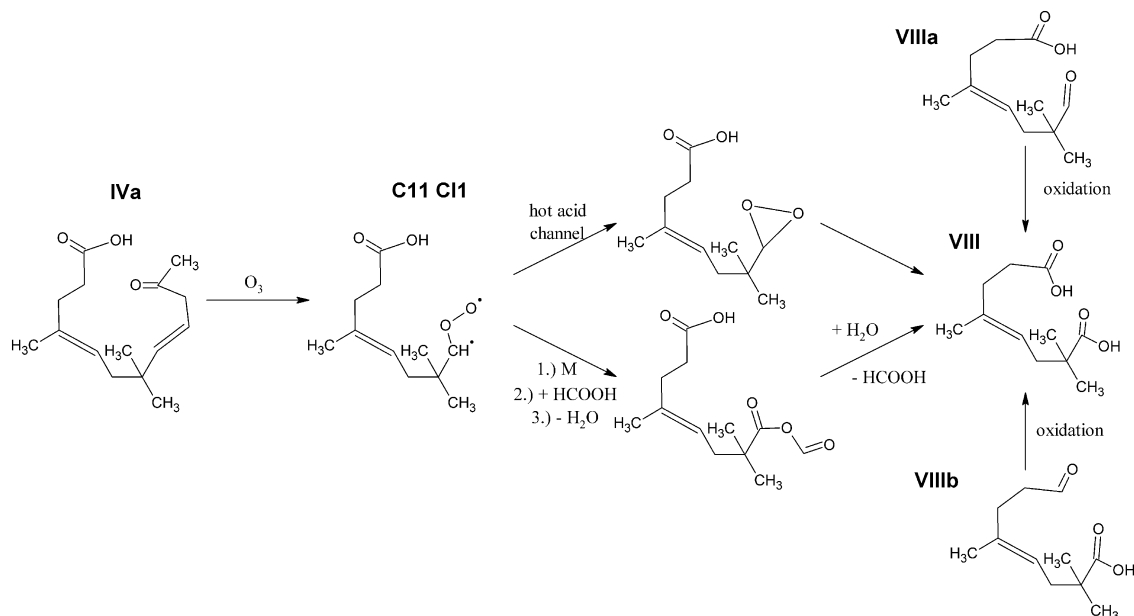


Fig. 13 Possible precursor pathways of X (C9-dicarboxylic acid).



Scheme 17

C10-oxocarboxylic acid **IXb**, but this molecule cannot easily lose CO because it is not an aldehyde. The CID spectra of the peak with the longer retention time can be explained without any problems with the structure of **IXb**. Both CID spectra are shown in Fig. 17.

The C9-dicarboxylic acid **X** was tentatively identified. One correlating peak was observed in the XICs of m/z 185 ($M - H^-$) and m/z 207 ($M + Na - 2H^-$). The α -humulene structure limited the number of possible products. Therefore it is suggested that **X** is the most probable C9-dicarboxylic acid. An interesting effect on the yield was observed upon the addition of water. It doubled the maximum yield and also seemed to stabilise the yield of the product, as can be seen in Fig. 18. Even with more than a twofold excess of ozone the

yield of the product remained almost constant. The reason of this observation is unknown. The effect of formic and acetic acids on the yield was not unambiguous. Cyclohexane lowered the yield, may be because of the loss of one oxidative species (OH-radicals). In Scheme 18 two possible pathways to form the C9-dicarboxylic acid **X** from C14-dicarboxylic acid **VId** are shown. Pathway W2 includes one oxidation reaction to form **X**, so the scavenging of the OH radical should reduce this oxidation channel.

Also in the XIC of m/z 185 a peak belonging to the C9-hydroxy-oxo-carboxylic acid **XI** was observed. The CID spectra showed the loss of water, CO, CO₂ and some combinations of those (see Fig. 19). The formation mechanism is displayed in reaction, Scheme 19, starting from the ozonolysis of the C15 oxo-carboxylic acid **III**.

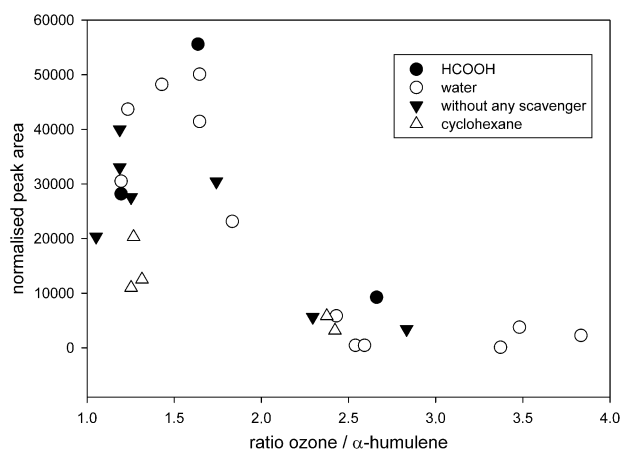


Fig. 14 Relative yield of VIII (C11-dicarboxylic acid) under various conditions.

The smallest molecules of the second generation that tentatively could be identified were the C8-hydroxy-oxocarboxylic acids **XIIa** and **XIIb**. The corresponding XIC of m/z 171 ($M - H^-$) showed two relevant signals at around 12.5 and 14 min (Fig. 20). The CID spectra of both peaks showed nearly the same fragment, showing the loss of CO, CO₂, water, but with different relative intensities of each fragment. Both products **XIIa** and **XIIb** can form each of these fragments, as is shown in Fig. 21. Because of the keto-enol-tautomerism the hydroxy- and the carbonyl-group can change their position in both molecules, what probably occurred in solution. In the case of **XIIa** the keto-form should be more preferred than in the case of **XIIb**, because of the conjugated π -system that is consequently formed. Therefore the intensity of the signals caused by the CO-loss should be lower in the CID spectra of **XIIa**. Also the fragment m/z 109 of **XIIa**, after the loss of H₂O and CO₂, should be less stable than that of **XIIb** (Fig. 21).

For these reasons the early peak should belong to **XIIa** and the late one to **XIIb**. The latter can be formed from the C14-dicarboxylic acid **Vc** (analogous Scheme 19). Starting from **Vb** analogous reactions led to the product **XIIa**.

3.6.3 Third-generation products. Only three C6-compounds (**XIII**, **XIVa** and **XIVb**) of the third-generation products could tentatively be identified by HPLC-MS. The C6-dicarboxylic acid **XIII**, with trivial name 2,2-dimethyl succinic acid, could positively be identified by comparison with reference material. The retention time of the signal from both the samples and the reference substance fully agreed, also the spectra of the CID experiments (loss of CO₂, H₂O and combination of both species). Both sodium-adducts ($M + Na - 2H^-$ at m/z 167 and $2M + Na - 2H^-$ at m/z 313) were also observed in the sample and the reference **XID**, showing identical fragmentation patterns. Incidentally, 2,2-dimethyl succinic acid is also known as a main product of the oxidative degradation of α -humulene in the liquid phase.⁵⁶ It is also a major product of the α -humulene gas phase ozonolysis.

Only one relative weak peak was observed in the XIC of m/z 129 ($M - H^-$) for the C6-oxocarboxylic acids **XIVa** and **XIVb**. It is very probable that a relatively large amount of this compound exists in the gas phase. The retention time was surprisingly shorter than that of the C6-dicarboxylic acid **XIII**, but it was longer than that of adipic acid. CID-experiments showed the loss of CO₂, CO (which is typical for aldehydes) and H₂O. It is suggested that both C6-oxocarboxylic acids are formed, but probably not with the same yield. These three third-generation products could originate from various known first- and second-generation products, as well from an unknown number of unidentified products. Three general possible pathways leading to the formation of **XIII**, **XIVa** and **XIVb** are shown in reaction in Scheme 20.

The postulated oxidation of the aldehydes is supported by the decreasing yield of **XIII** upon the addition of cyclohexane.

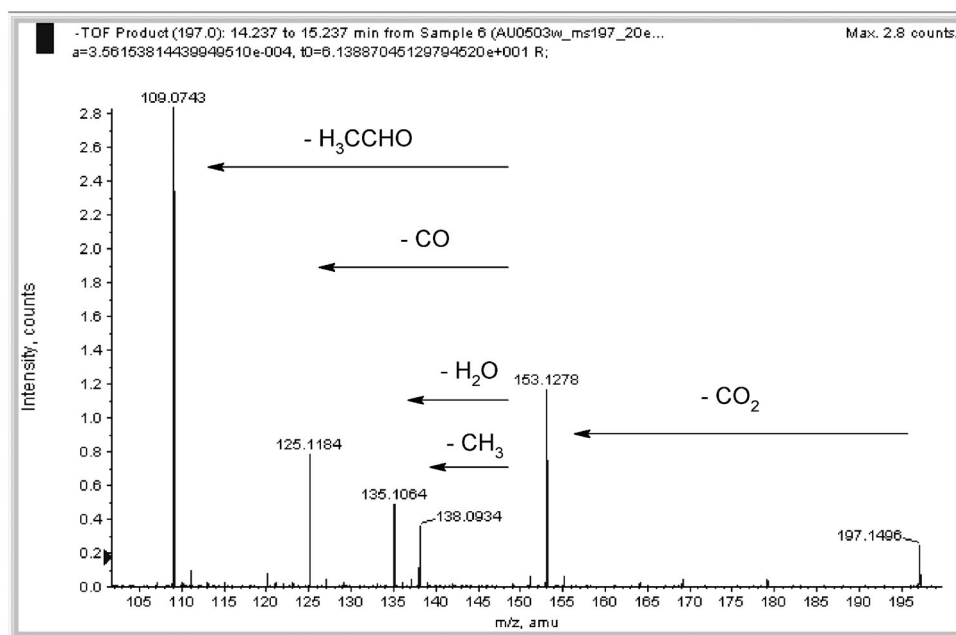


Fig. 15 CID mass spectra of m/z 197 at 14.7 min (C11-oxocarboxylic acids **VIIIa** and **VIIIb**).

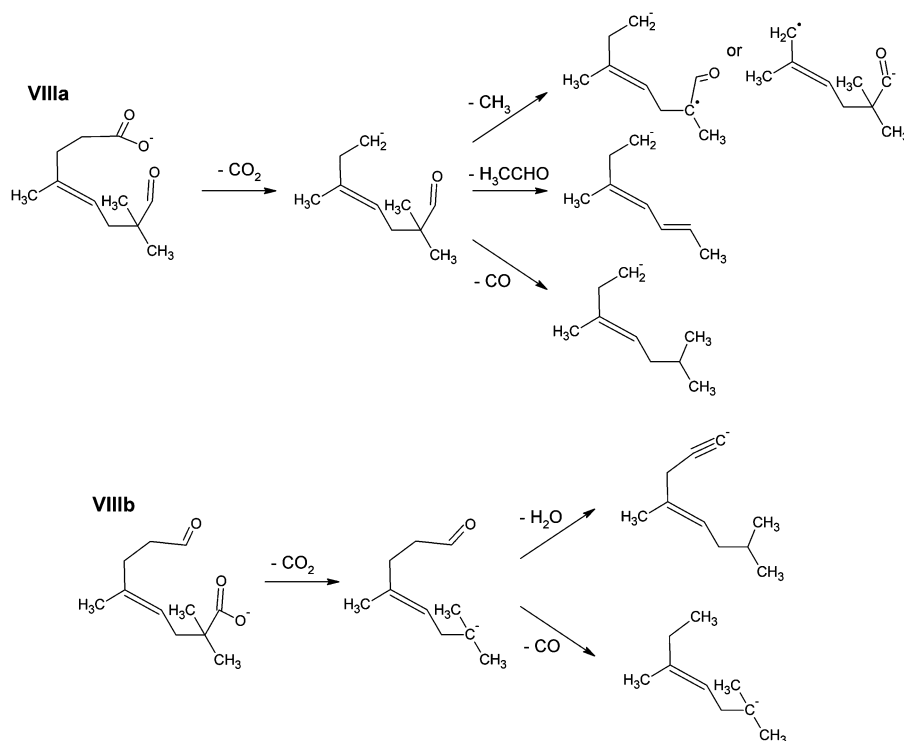


Fig. 16 CID fragmentation patterns of VIIa and VIIb (C11-oxocarboxylic acids).

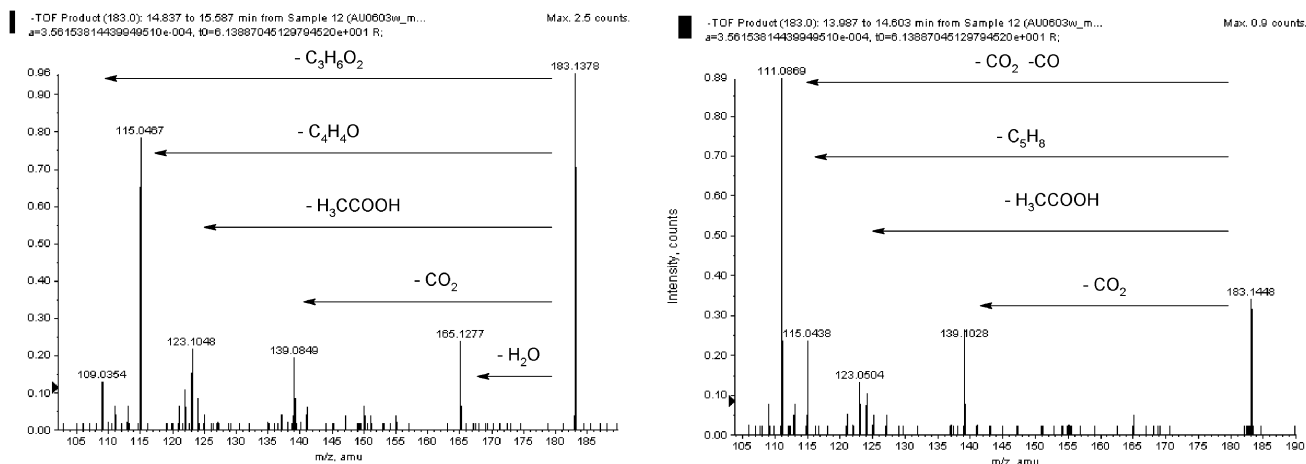


Fig. 17 CID of m/z 183 (C10-oxocarboxylic acid); left frame: late peak (IXb); right frame: early peak (IXa).

In addition, an interesting effect of the addition of CI-scavengers was also observed for the C6-dicarboxylic acid **XIII**. The addition of H_2O caused the yield slightly to decrease, whereas the formic and acetic acid caused the yield to increase. The signal of **XIVa** and **XIVb** was too weak to estimate the effects of the different scavengers.

No other small compounds could be identified with the HPLC-MS, but some indications of the presence of smaller molecules were seen with the PTR-MS technique. Without any chromatographic separation and without the possibility of performing MS/MS experiments, the clear identification of the compounds is very difficult. Scheme 21 is showing the most probable observed dicarbonyl products (**XV**, **XVII** and **XIX**). Other compounds producing equal mass-charge-ratios are

possible and probable. The same issues are even more valid for the oxocarboxylic acids **XVI** and **XVIII**. The products of the third generation are shown in Table 6, including the probability of their identification. The relative yields of the dicarbonyl products **XIX** (m/z 87, full circles), **XVII** (m/z 101, dotted circles) and **XV** (m/z 115, triangles) are shown in Fig. 22. Only the relative yields are shown because no calibrations for these compounds were performed. It is not excluded that isomeric compounds were formed. It is also possible that other formed compounds have fragments with the same mass to charge ratio. For the interpretation of the signals it was assumed that in the considered concentration range the correlation of the signal intensity and the concentration is almost linear. As seen in Fig. 22 the yield of the three

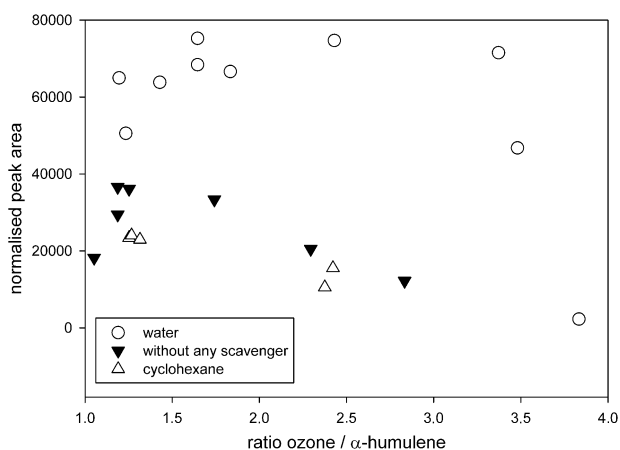


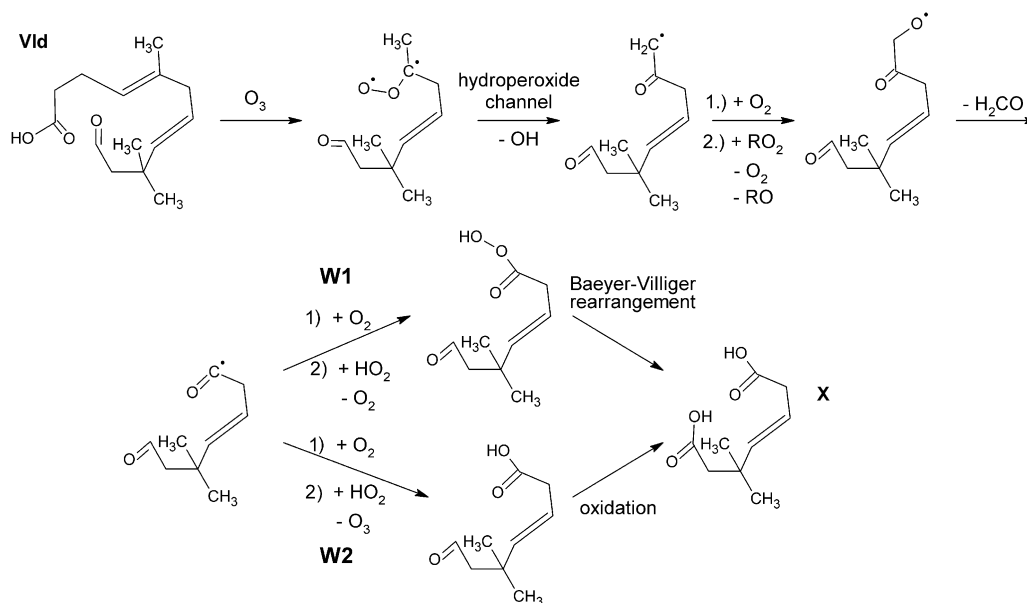
Fig. 18 Relative yield of **X** (C9-dicarboxylic acid) under various conditions.

dicarbonyl compounds increased generally with higher ozone excess (the α -humulene mixing ratios of the experiments

were comparable). An excess of α -humulene led to a relatively low yield of the three dicarbonyl compounds. The 1.7-fold excess of ozone increased the signal intensity of all compounds, especially the one of C5 compound **XVII**. High excess of ozone led to a much higher yield of **XV** (C6) and also **XIX** (C4), but only to a slightly increased yield of **XVII** (C5), compared to the yields of 1.7-fold excess ozone. Because of the different ionization efficiencies of the substances the absolute signal intensities do not indicate which compound has the highest or lowest mixing ratio.

4. Conclusions

Various aspects of ozonolysis of α -humulene have been investigated, including the kinetics of ozone with the three double bonds, the determination of the yield of OH radicals, the formation of secondary ozonides, the production of secondary aerosols and the tentative identification of a variety of the three generation products. The gas phase ozonolysis was studied under various experimental conditions, including the



Scheme 18

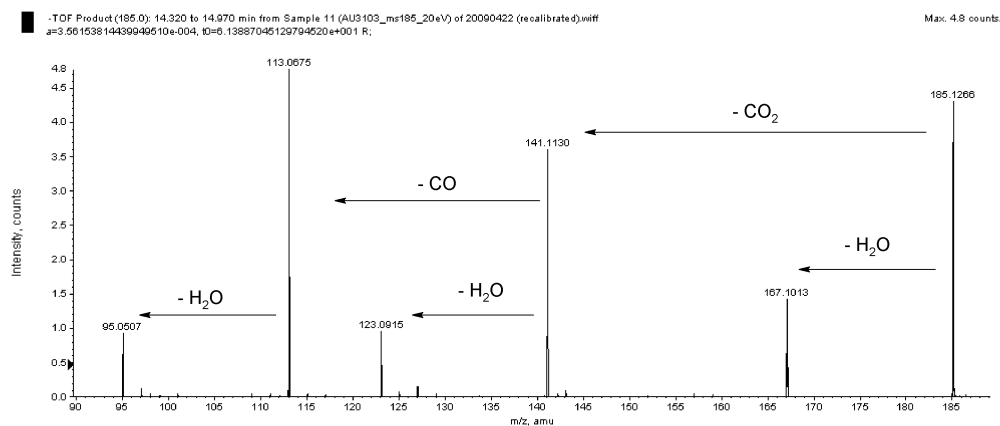
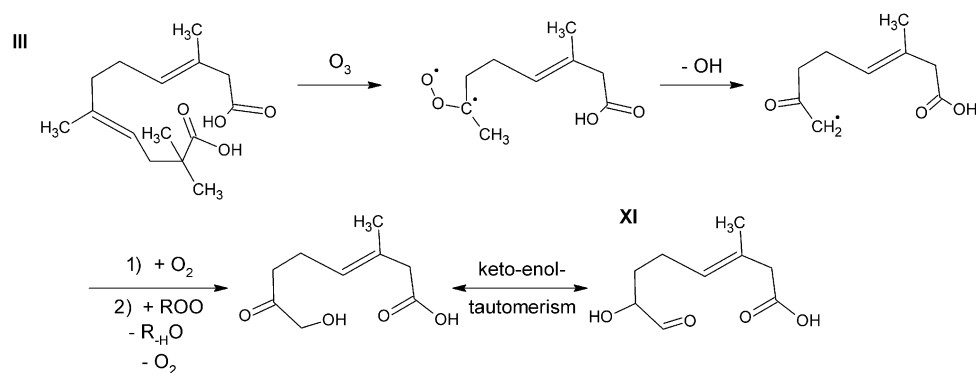
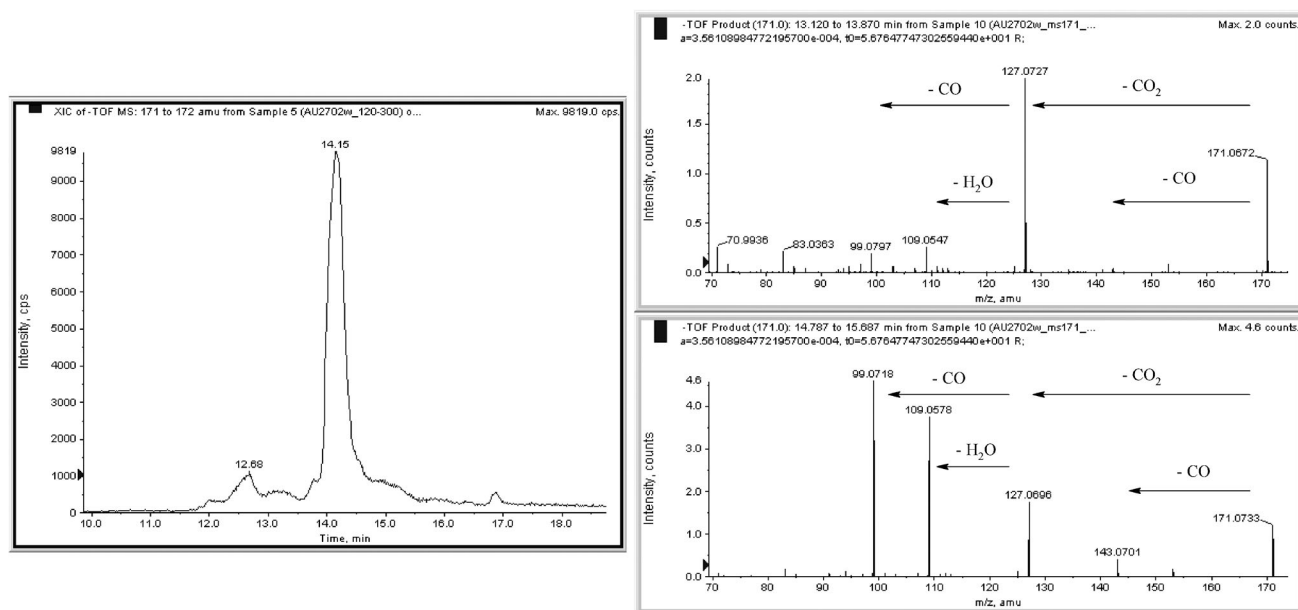
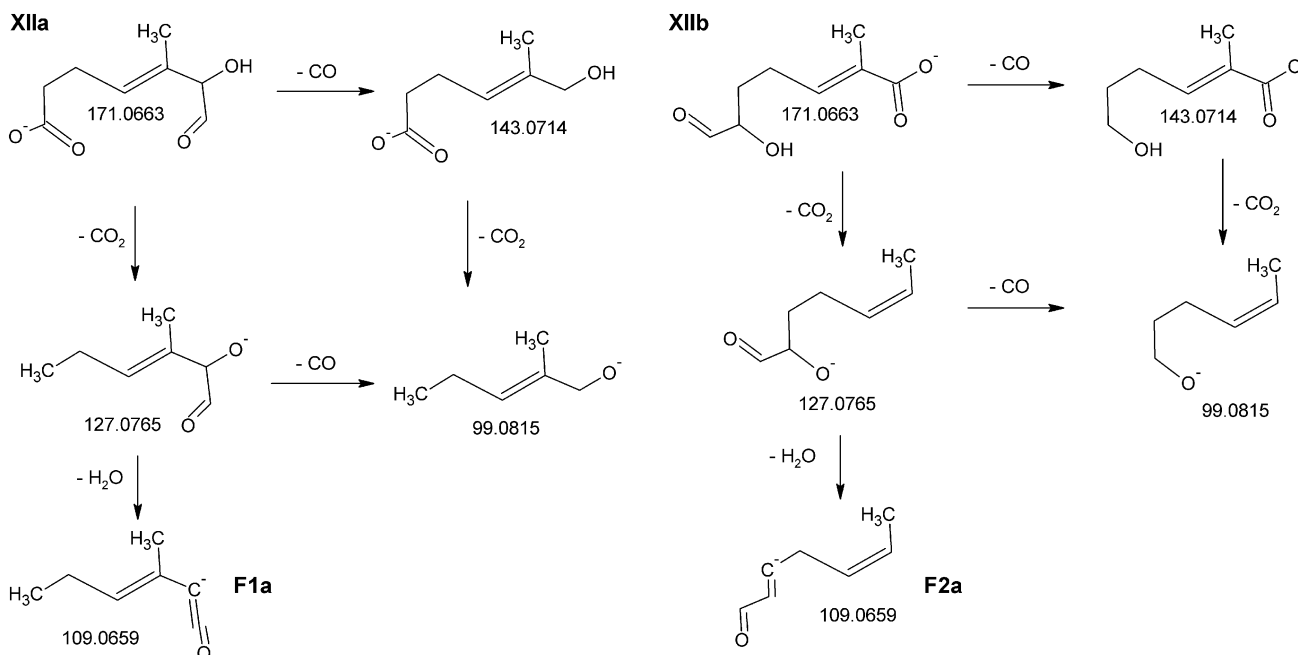
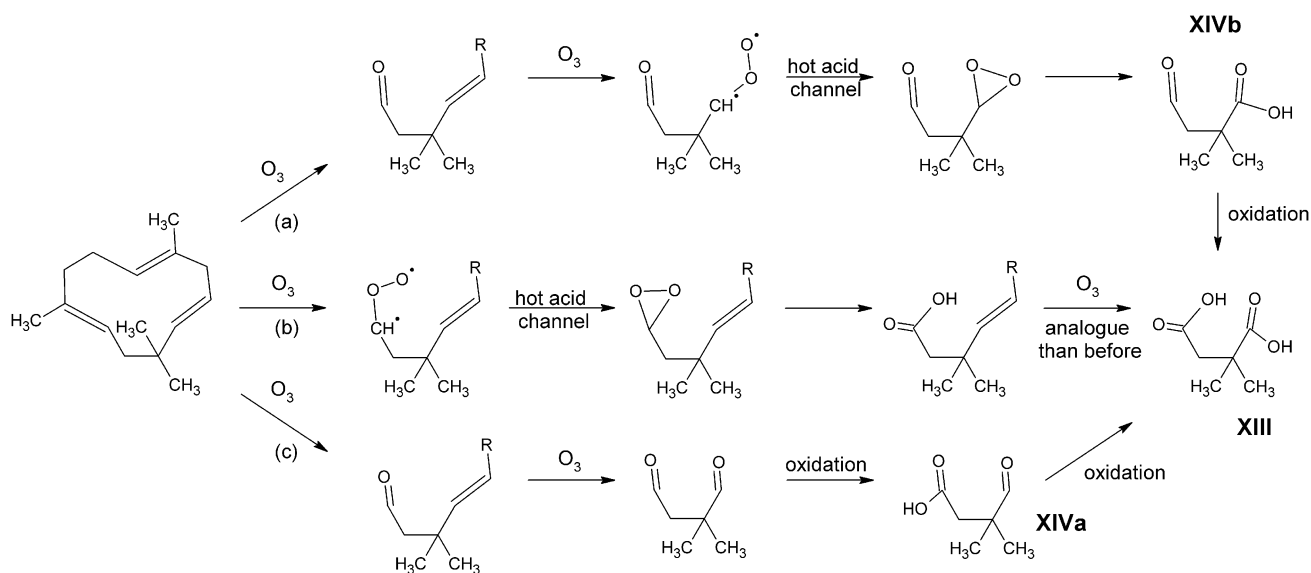


Fig. 19 CID spectra of **XI** (C9-hydroxy-oxocarboxylic acid).

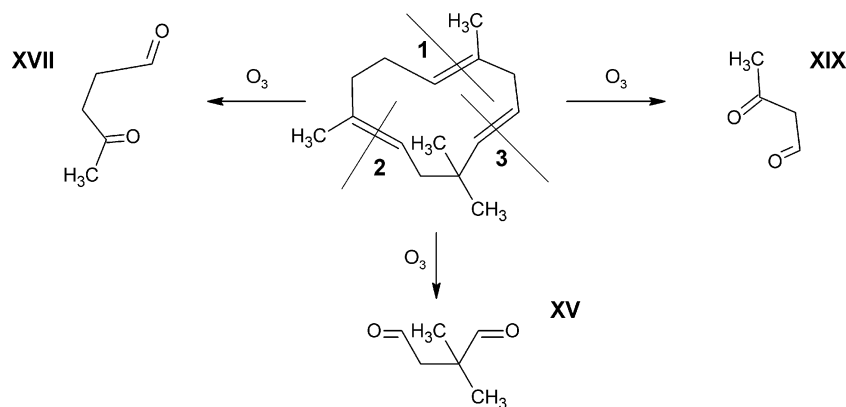


Scheme 19

Fig. 20 XIC of *m/z* 171 (C8-hydroxy-oxocarboxylic acids **XIIa** and **XIIb**) and CID of correlated peaks.Fig. 21 Fragmentation pattern of **XIIa** and **XIIb** (C8-hydroxy-oxocarboxylic acids).



Scheme 20



Scheme 21

addition of cyclohexane as an OH-radical scavenger and HCOOH, CH₃COOH and H₂O as CI-scavengers, and the variation of the α -humulene to ozone ratio.

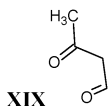
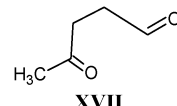
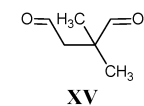
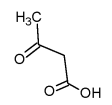
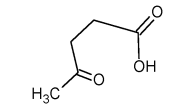
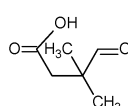
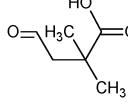
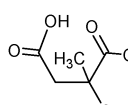
A striking result was the detection by FTIR of secondary ozonides (SOZ) in the gas phase. More important, the addition of CI-scavengers, such as HCOOH and H₂O, had not a significant effect on their formation. In a nearly ozone-free environment the SOZs remained relatively stable. Only about 20% of the SOZs was degraded after 90 min with a dew point below 193 K (−80 °C). However, 40% of the SOZs remained after more than two hours with a humidity of about 30%. Evidence was found that ozone destroyed the SOZs. In experiments with more than twofold excess of ozone, the SOZ was degraded very fast; in most cases no SOZ was detectable after few minutes.

The observed stability of the secondary ozonides provides important fundamental insight in their unimolecular formation. SOZs are formed by the intramolecular reaction of the Criegee moiety with the carbonyl group. This suggests that during the ozonolysis of α -humulene at atmospheric pressures the initially formed POZ will decompose rapidly giving excited Criegee Intermediates. A large fraction of the excited CI will be

stabilized and react intramolecularly to form stable SOZ, while the formation of OH-radicals *via* the hydroperoxide channel will be a minor process. The results obtained in this study support the theoretical calculations by Chuong *et al.*,⁴³ who predict that the ozonolysis of C15 endocyclic alkenes will dominantly produce secondary ozonides.

Kinetic experiments provided an average rate coefficient for the first-generation products (second DB) of $k_1 = (3.6 \pm 0.9) \times 10^{-16} \text{ cm}^3 \text{ molecule}^{-1} \text{ s}^{-1}$; this means more than 30 times slower than for the reaction of ozone with the first DB ($k_1 = 1.17 \times 10^{-14} \text{ cm}^3 \text{ molecule}^{-1} \text{ s}^{-1}$). The second-generation products (third DB) have an average rate coefficient of $k_2 = (3.0 \pm 0.7) \times 10^{-17} \text{ cm}^3 \text{ molecule}^{-1} \text{ s}^{-1}$; they are at average 12 times slower than the reaction of ozone with the first-generation products and nearly 400 times slower than with the first DB of α -humulene. At typical tropospheric ozone mixing ratios of 30 ppb the lifetime of α -humulene is about 2 min,⁴⁸ whereas the first- and second-generation products have average lifetimes of 1 h and 12.5 h, respectively. The ozonolysis of the first-generation products is still faster than the one of the sesquiterpenes α -copaene (2.5 h lifetime) and the monoterpenes α -pinene and sabinene (4.3 h), 3-carene (10 h)

Table 6 Identification of third-generation products

Compound class	C4	C5	C6	Identification
Dicarbonyl	 XIX	 XVII	 XV	Evidence from PTR-MS
Carbonyl carboxylic acids part 1	 XVIII	 XVI		Hints by PTR-MS
Carbonyl carboxylic acids part 2			 XIVa  XIVb	Tentatively identified by HPLC-MS
Dicarboxylic acids			 XIII	Identified by HPLC-MS with reference

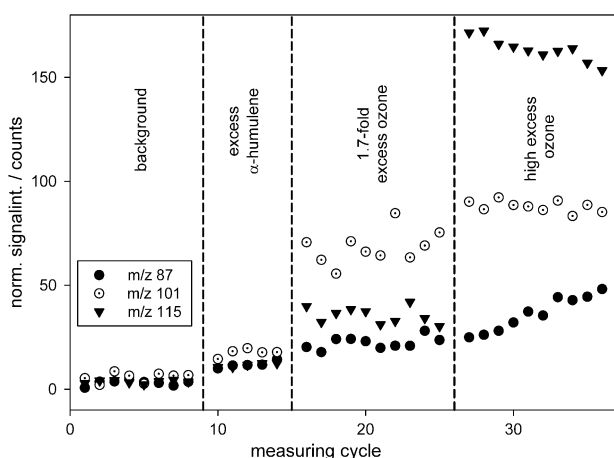


Fig. 22 Quasi-molecular ion signals of **XIX** (m/z 87), **XVII** (m/z 101) and **XV** (m/z 115): displayed are examples of background signal, and conditions of excess of α -humulene (2.5 : 1), 1.7-fold excess of ozone, and high excess of ozone (taken from three different experiments).

and β -phellandrene (7.9 h). Even the average lifetime of second-generation products is with 12.5 h shorter than that of the sesquiterpenes α -cedrene (14 h) and the monoterpene β -pinene (24.7 h).^{23,48}

The OH-radical yield was determined *via* the yield of cyclohexanone measured by PTR-MS. OH yields of $(10.5 \pm 0.7)\%$ for the first double bond and $(12.9 \pm 0.7)\%$ for the second double bond could be calculated from the measurement data. Thus it can be concluded that, first the hydroperoxide channel is not the major process, and second the ozonolysis

of α -humulene is a minor source of OH-radicals in the troposphere.

SOA yields have been also determined. In the case of 4-fold excess of ozone nearly 45% SOA yield was obtained. α -Humulene in excess lowered the yield to about 14 to 17%. In the first case the SOA is properly dominated by second- and third-generation products, while the excess of α -humulene caused the formation of most first-generation products.

Products of all three product generations could tentatively be identified: those of the first-generation contained 13 to 15 carbon atoms, those of the second-generation 8 to 11 and those of the third-generation 4 to 6. Because of the unavailability of reference substances only the C6-dicarboxylic acid **XIII** (2,2-dimethyl-succinic acid) could be positively identified by comparison with an authentic standard.

The PTR-MS measurements allowed investigating on-line the progress of the ozonolysis of α -humulene in the reactor. Besides the measurement of cyclohexane only some third-generation products could be tentatively identified. All C4- and C5-compounds could only be observed in the gas-phase, also the C6-dicarbonyl compound **XV**. The three other tentatively identified third-generation products could only be observed in the aerosol phase, which was investigated by HPLC-ESI(–)-MS. The focus in this part of the study was laid on the carboxylic acids and the experimental setup was optimised for this class of compounds. Therefore only carboxylic acids could be identified with this technique. As mentioned above, the C6-dicarboxylic acid **XIII** could definitely be identified, the corresponding oxocarboxylic acids **XIVa** and **XIVb** only tentatively. In total eight products of the third-generation could be tentatively identified.

The second-generation products possessed between 8 and 11 carbon atoms; only compounds with a carboxylic acid group could be detected. The C11- and C9- dicarboxylic acids, respectively, **VIII** and **X**, were tentatively identified. Only for the C11-compound both structural corresponding oxocarboxylic acids (**VIIIa+b**) were also observed. A C10-dicarboxylic acid could not be identified, although the C10-oxocarboxylic acid **IXa** is structurally very similar to the corresponding C11-compound **VIIIa**. The other tentatively identified C10-oxocarboxylic acid **IXb** contained another remaining double bond (DB3). Three compounds in this generation are hydroxy-oxocarboxylic acids, two contained 8 carbon atoms (**XIIa+b**) and one 9 carbon atoms (**XI**). Moreover, these three compounds have the same functional groups and are also the only compounds with DB1 as remaining double bond. In total 9 products of the second generation could be tentatively identified, two are dicarboxylic acids, four oxocarboxylic acids and three having an additional hydroxyl-group.

In total 25 products of the first-generation could be tentatively identified, containing between 13 and 15 carbon atoms. Because of the very similar structures of many postulated compounds the clear assignment of the peaks was not always possible for the first-generation products. Only first-generation dicarboxylic acids could be identified, which possessed an additional oxo-group (C15, **IIa+b**). Also the C15-dicarboxylic acid **III** could tentatively be identified. In this study 8 possible C15-hydroxy-oxocarboxylic acids were postulated (**IIIa-h**). The four tentatively identified C15-oxocarboxylic acids (**IVa-d**) and the dicarboxylic acid **III** were also observed in the photooxidation study by Jaoui and Kamens.¹⁹ Three C14-dicarboxylic acids (**Va-c**) and five C14-oxocarboxylic acids (**VIa-e**) were tentatively identified, including those oxocarboxylic acids which are suggested to be precursor substance to the dicarboxylic acids. Both observed C13-compounds are dicarboxylic acids.

In total 37 compounds in the aerosol phase and five compounds in the gas phase could be tentatively identified. The relative yields of these products could be influenced by the different scavengers. Cyclohexane as an OH-scavenger had rarely a positive effect on the yield, but it lowered the yield of some products up to 40%. The CI scavengers increased the yield of some products up to factor 3. But there seems to be no general influence of the different scavenger on the products yield.

Conclusively, this comprehensive study on the ozonolysis of α -humulene reveals new fundamental information on the stability of secondary ozonides, which are formed by rapid unimolecular formation of the Criegee Intermediates. Because of their stability, SOZ formation must be considered as a major reaction product, whereas the OH formation (10%) via the hydroperoxy channel will be a minor product channel. Most assigned products in the particle phase have been derived from the organic coproduct formed simultaneously with the OH radical. The hot acid channel proved to have a minor contribution to the tentatively identified products.

Acknowledgements

This research was partly carried out in the frame of the BELSPO SSD project "IBOOT" (contract SD/AT/03A). The authors thank Christoph B. M. Groß for performing

sensitivity calculations in the simulations of the kinetic parameters.

Notes and references

- 1 Y. Shu and R. Atkinson, *Int. J. Chem. Kinet.*, 1994, **26**, 1193–1205.
- 2 A. Guenther, C. N. Hewitt, D. Erickson, R. Fall, C. Geron, T. Graedel, P. Harley, L. Klinger, M. Lerdau, W. A. McKay, T. Pierce, B. Scholes, R. Steinbrecher, R. Tallamraju, J. Taylor and P. Zimmerman, *J. Geophys. Res.*, 1995, **100**, 8873–8892.
- 3 J. E. Saxton, A. C. Lewis, J. H. Kettlewell, M. Z. Ozel, F. Gogus, Y. Boni, S. O. U. Korogone and D. Serca, *Atmos. Chem. Phys.*, 2007, **7**, 4095–4106.
- 4 M. Karl, K. Tsigaridis, E. Vignati and F. Dentener, *Atmos. Chem. Phys.*, 2009, **9**, 7003–7030.
- 5 R. J. Griffin, D. R. Cocker, R. C. Flagan and J. H. Seinfeld, *J. Geophys. Res.*, 1999, **104**, 3555–3567.
- 6 M. Kanakidou, J. H. Seinfeld, S. N. Pandis, I. Barnes, F. J. Dentener, M. C. Facchini, R. van Dingenen, B. Ervens, A. Nenes, C. J. Nielsen, E. Swietlicki, J. P. Putaud, Y. Balkanski, S. Fuzzi, J. Horth, G. K. Moortgat, R. Winterhalter, C. E. L. Myhre, K. Tsigaridis, E. Vignati, E. G. Stephanou and J. Wilson, *Atmos. Chem. Phys.*, 2005, **5**, 1053–1123.
- 7 B. Bonn, A. Hirsikko, H. Hakola, T. Kurten, L. Laakso, M. Boy, M. Dal Maso, J. M. Makela and M. Kulmala, *Atmos. Chem. Phys.*, 2007, **7**, 2893–2916.
- 8 S. Kim, T. Karl, D. Helmig, R. Daly, a. R. Rasmussen and A. Guenther, *Atmos. Meas. Tech.*, 2009, **2**, 99–112.
- 9 T. Sakulyanontvittaya, A. Guenther, D. Helmig, J. Milford and C. Wiedinmyer, *Environ. Sci. Technol.*, 2008, **42**, 8784–8790.
- 10 D. Helmig, J. Ortega, T. Duhl, D. Tanner, A. Guenther, P. Harley, C. Wiedinmyer, J. Milford and T. Sakulyanontvittaya, *Environ. Sci. Technol.*, 2007, **41**, 1545–1553.
- 11 T. R. Duhl, D. Helmig and A. Guenther, *Biogeosciences*, 2008, **5**, 761–777.
- 12 F. Chen, D. Tholl, J. D'Auria, A. Farooq, E. Pichersky and J. Gershenzon, *Plant Cell*, 2003, **15**, 481–494.
- 13 P. Ciccioli, E. Brancaleoni, M. Frattoni, V. Di Palo, R. Valentini, G. Tirone, G. Seufert, N. Bertin, U. Hansen, O. Csiky, R. Lenz and M. Sharma, *J. Geophys. Res.*, 1999, **104**, 8077–8094.
- 14 D. Degenhardt and D. Lincoln, *J. Chem. Ecol.*, 2006, **32**, 725–743.
- 15 C. De Moraes, M. Mescher and J. Tumlinson, *Nature*, 2001, **410**, 577–580.
- 16 G. Schuh, A. Heiden, T. Hoffmann, J. Kahl, P. Rockel, J. Rudolph and J. Wildt, *J. Atmos. Chem.*, 1997, **27**, 291–318.
- 17 S. T. Katsiotis, C. R. Langezaal and J. J. C. Scheffe, *Planta Med.*, 1989, **55**, 634.
- 18 K. E. Huff Hartz, T. Rosenorn, S. R. Ferchak, T. M. Raymond, M. Bilde, N. M. Donahue and S. N. Pandis, *J. Geophys. Res.*, 2005, **110**, 14208–14216.
- 19 M. Jaoui and R. M. Kamens, *J. Atmos. Chem.*, 2003, **46**, 29–54.
- 20 A. Lee, A. H. Goldstein, J. H. Kroll, N. L. Ng, V. Varutbangkul, R. C. Flagan and J. H. Seinfeld, *J. Geophys. Res.*, 2006, **111**, 1–25.
- 21 M. Dekermenjian, D. Allen, R. Atkinson and J. Arey, *Aerosol Sci. Technol.*, 1999, **30**, 349–363.
- 22 P. Neeb, O. Horie and G. K. Moortgat, *J. Phys. Chem.*, 1998, **102**, 6778–6785.
- 23 R. Winterhalter, F. Herrmann, B. Kanawati, T. L. Nguyen, J. Peeters, L. Vereecken and G. K. Moortgat, *Phys. Chem. Chem. Phys.*, 2009, **11**, 4152–4172.
- 24 M. Finkbeiner, P. Neeb, O. Horie and G. K. Moortgat, *Fresenius' J. Anal. Chem.*, 1995, **351**, 521–525.
- 25 W. Lindinger, A. Hansel and A. Jordan, *Int. J. Mass Spectrom. Ion Processes*, 1998, **173**, 191–241.
- 26 S. Taddei, P. Toscano, B. Gioli, A. Matese, F. Miglietta, F. P. Vaccari, A. Zaldei, T. Custer and J. Williams, *Environ. Sci. Technol.*, 2009, **43**, 5218–5222.
- 27 F. Herrmann, R. Winterhalter, G. K. Moortgat and J. Williams, *Atmos. Environ.*, 2010, **44**, 3458–3464.
- 28 A. Römpf, *PhD thesis*, Johannes Gutenberg University, Mainz, 2003.
- 29 A. Sadezky, R. Winterhalter, B. Kanawati, A. Römpf, B. Spengler, A. Mellouki, G. Le Bras, P. Chaimbault and G. K. Moortgat, *Atmos. Chem. Phys.*, 2008, **8**, 2667–2699.

- 30 R. Atkinson, *J. Phys. Chem. Ref. Data*, 1997, **26**, 215–290.
- 31 A. R. Curtis and W. P. Sweetenham, *AERE Report R 12808*, Harwell Laboratory, Oxfordshire, 1987.
- 32 R. Van Dingenen, F. Raes and H. Vanmarcke, *J. Aerosol Sci.*, 1989, **20**, 113–122.
- 33 J. R. Pierce, G. J. Engelhart, L. Hildebrandt, E. A. Weitkamp, R. K. Pathak, N. M. Donahue, A. L. Robinson, P. J. Adams and S. N. Pandis, *Aerosol Sci. Technol.*, 2008, **42**, 1001–1015.
- 34 L. Hildebrandt, N. M. Donahue and S. N. Pandis, *Atmos. Chem. Phys.*, 2009, **9**, 2973–2986.
- 35 B. Bonn, *PhD thesis*, Johannes Gutenberg University, Mainz, 2002.
- 36 F. Herrmann, *Master thesis*, Johannes Gutenberg University, Mainz, 2006.
- 37 N. M. Donahue, K. E. Huff Hartz, B. Chuong, A. A. Presto, C. O. Stanier, T. Rosenhorn, A. L. Robinson and S. N. Pandis, *Faraday Discuss.*, 2005, **130**, 295–309.
- 38 B. K. Pun and C. Seigneur, *Atmos. Chem. Phys.*, 2007, **7**, 2199–2216.
- 39 J. H. Kroll and J. H. Seinfeld, *Atmos. Environ.*, 2008, **42**, 3593–3624.
- 40 J. G. Calvert, R. Atkinson, J. A. Kerr, S. Madronich, G. K. Moortgat, T. J. Wallington and G. Yarwood, *The mechanisms of atmospheric oxidation of the alkenes*, Oxford University Press, 2000.
- 41 D. Cremer, J. Gauss, E. Kraka, J. F. Stanton and R. J. Bartlett, *Chem. Phys. Lett.*, 1993, **209**, 547–556.
- 42 D. Johnson and G. Marston, *Chem. Soc. Rev.*, 2008, **37**, 699–716.
- 43 B. Chuong, J. Y. Zhang and N. M. Donahue, *J. Am. Chem. Soc.*, 2004, **126**, 12363–12373.
- 44 R. Atkinson, S. M. Aschmann, J. Arey and B. Shorees, *J. Geophys. Res.*, 1992, **97**, 6065–6073.
- 45 T. Berndt, O. Böge and F. Stratmann, *Atmos. Environ.*, 2003, **37**, 3933–3945.
- 46 R. Atkinson and S. M. Aschmann, *Environ. Sci. Technol.*, 1993, **27**, 1357–1363.
- 47 R. Atkinson, *J. Phys. Chem. Ref. Data*, 1989, **Monograph 1**, 1–246.
- 48 Y. Shu and R. Atkinson, *J. Geophys. Res.*, 1995, **100**, 7275–7275.
- 49 R. Bariseviciute, J. Ceponkus, A. Gruodis and V. Sablinskas, *Cent. Eur. J. Chem.*, 2006, **4**, 578–591.
- 50 R. Fajgar, J. Vitek, Y. Haas and J. Pola, *J. Chem. Soc., Perkin Trans.*, 1999, **2**, 239–248.
- 51 R. Winterhalter, P. Neeb, D. Grossmann, A. Kolloff, O. Horie and G. K. Moortgat, *J. Atmos. Chem.*, 2000, **35**, 165–197.
- 52 J. Park, A. L. Gomez, M. L. Walser, A. Lin and S. A. Nizkorodov, *Phys. Chem. Chem. Phys.*, 2006, **8**, 2506–2512.
- 53 R. G. Bulgakov, E. Y. Nevyadovsky, Y. G. Ponomareva, D. S. Sabirov, V. P. Budtov and S. D. Razumovskiic, *Russ. Chem. Bull.*, 2005, **54**, 2468–2470.
- 54 H. E. Seyfarth, I. Anger and A. Rieche, *J. Prakt. Chem.*, 1968, **311**, 147–152.
- 55 N. N. Nichols, L. N. Sharma, R. A. Mowery, C. K. Chambliss, G. P. van Walsum, B. S. Dien and L. B. Iten, *Enzyme Microb. Technol.*, 2008, **42**, 624–630.
- 56 D. E. Cane, *Chem. Rev.*, 1990, **90**, 1089–1103.